Dynamics and Kinematics of the Laying and Recovery of Submarine Cable

By E. E. ZAJAC

(Manuscript received June 5, 1957)

This paper is an attempt to formulate a comprehensive theory with which the forces and motions of a submarine cable can be determined in typical laying and recovery situations. In addition to the fundamental case of a cable being laid or recovered with a ship sailing on a perfectly calm sea over a horizontal bottom, the effects of ship motion, varying bottom depth, ocean cross currents, and the problem of cable laying control are considered. Most of the results reduce to simple formulas and graphs. Their application is illustrated by examples.

TABLE OF CONTENTS

	Page
I. Introduction	1132
II. Basic Assumptions	1133
III. Two-Dimensional Stationary Model	1134
3.1 General	1134
3.2 Normal Drag Force and the Cable Angle α	1135
3.3 Tangential Drag Force	1139
3.4 Sinking Velocities and Their Relationship to Drag Forces	1141
3.5 General Solution of the Stationary Two-Dimensional Model	1143
3.6 Approximate Solution for Cable Laying	1146
3.7 Approximate Solution for Cable Recovery	1149
3.8 Shea's Alternative Recovery Procedure	1153
IV. Effects of Ship Motions	1154
4.1 Tensions Caused by Ship Motions	1154
V. Deviations from a Horizontal Bottom	1158
5.1 Kinematics of Laying Over a Bottom of Varying Depth	1158
5.2 Time-Wise Variation of the Mean Tension in Laying Over a Bottom of Varying Depth	1161
5.3 Residual Suspensions	1163
VI. Cable Laying Control	1165
6.1 General	1165
6.2 Accuracy of the Piano Wire Technique	1166
VII. Three-Dimensional Stationary Model	1169
7.1 General	1169
7.2 Perturbation Solution for a Uniform Cross-Current	1172
Appendix A. Discussion of the Two-Dimensional Stationary Configuration for Zero Bottom Tension	1175
Appendix B. Computation of the Transverse Drag Coefficient and the Hydrodynamic Constant of a Smooth Cable from Published Data	1177

Appendix C. Some Approximate Solutions for Laying and Recovery 1180
C.1 Laying 1180
C.2 Recovery 1183
Appendix D. Analysis of the Effect of Ship Motion 1184
D.1 Formulation of the Differential Equations 1184
D.2 Perturbation Equations 1187
D.3 Solution of the Perturbation Equations 1189
D.4 Transverse Response 1190
D.5 Second-Order Longitudinal Response 1191
D.6 Numerical Results 1194
Appendix E. Tension Rise with Time for Suspended Cable 1195
E.1 Formulation of the Solution of the Problem 1195
E.2 Nomograph for the Solution of Equation (99) 1198
E.3 Numerical Example 1199
Appendix F. The Three-Dimensional Stationary Model 1202
F.1 Derivation of the Differential Equations 1202
F.2 Perturbation Solution for a Uniform Cross Current 1204
Acknowledgments 1206
References 1206

Glossary of Symbols

A	Amplitude of harmonic ship motion
c_1 , c_2 , $\bar{c}_2$	Longitudinal wave velocity; transverse wave velocity in air and water
C_D , C_f	Transverse and tangential drag coefficients
d	Cable diameter, also distance behind the ship at which the cable enters the lower stratum
D_N , D_T	Normal and tangential unit drag forces
e	Sidewise distance from the laid cable to the ship
$\overline{EA}$	Extensile rigidity
h	Ocean depth
$\bar{h} = \frac{wh}{\overline{EA}}$	Dimensionless ocean depth
H	Hydrodynamic constant
L	Inclined cable length from surface to bottom, also from ship to surface
N_R	Reynolds number
p, q	Longitudinal and transverse deviational cable displacements
P_0 , Q_0	Longitudinal and transverse ship displacements

P_1	Deviation from mean pay-out or haul-in rate
S, X	Arc length and horizontal distance from the touchdown point to the ship
$\bar{S} = \frac{S}{h}, \quad \bar{X} = \frac{X}{h}$	Dimensionless forms of S and X
t	Time
$\bar{t} = \frac{Vt}{h}$	Dimensionless time
T, T_s, T_0	Cable tension at an arbitrary point, at the ship, and at the bottom
$\overline{T} = \frac{T}{wh}, \quad \overline{T}_s = \frac{T_s}{wh}, \quad \overline{T}_0 = \frac{T_0}{wh}$	Dimensionless forms of T, T_s and T_0
T_p, T_q	Cable tension due to longitudinal and transverse ship motion
V, V_c	Ship speed, pay-out or haul-in rate
V_N, V_T	Normal and tangential velocity of the water relative to the cable configuration
V_t	Tangential velocity of the water relative to a cable element
w, w_a	Submerged and in-air unit cable weight
α, α_0	Critical angle, approximate critical angle
α_s	Cable angle at the surface
β	Descent angle, cross current orientation (Section 7.1)
$\gamma = \frac{2 - \sin^2 \alpha}{\sin^2 \alpha}$	Constant, also ascent angle
ϵ	Slack
θ	Orientation of a cable element
θ, ψ	Spherical polar coordinates for the three-dimensional model
κ, λ	Constants (see Appendix C)

$\Lambda = \frac{C_D \rho d V^2}{2} = \frac{\cos \alpha}{\sin^2 \alpha}$	Constant
μ, ν	Constants
ν	Kinematic viscosity
ξ, η, ζ	Rectangular coordinates for the three-dimensional model
ρ	Mass density of water
ρ_c , ρ_w	Mass per unit length of cable in air and water
ϕ	Deviation from the stationary angle, also angle between ξ axis and $\vec{V}$ (Section 7.1)

I. INTRODUCTION

In the summer of 1857, the first attempted laying of a transatlantic cable ended dismally when, after only a few hundred miles had been laid, the cable broke and fell into the sea. Although fouling of the pay-out gear caused by a negligent workman was the principal suspected reasons for the failure, its occurrence aroused great interest in the detailed dynamics and kinematics of the laying of submarine cable, and leading British scientists such as Kelvin and Airy published analyses of this problem in late 1857 and early 1858.[1, 2, 3, 4, 5]

However, after this initial activity, interest in submarine cable dynamics and kinematics evidently waned for there appear only sporadic subsequent investigations in the literature.[6, 7, 8, 9, 10] Further, the results of the early and subsequent analytical investigations have been, by and large, little utilized in cable laying and recovery practice. One can conjecture several reasons for this. For one, because the early analytical work was done before the advent of modern hydrodynamic theory, it did not rest on a secure base. Thus, as late as 1875, one finds vigorous debate over the nature of the tangential resistance of water to the cable.[9] For another, the results of the analyses could not all be expressed in terms of elementary functions and required the numerical evaluation of some definite integrals. In the 1850's this was a tedious and laborious process. However, these are probably secondary reasons. For, after another failure in the early summer of 1858, a transatlantic cable was successfully laid in August of that year. The mechanical problem of depositing a cable was thus proved surmountable without complicated mathematical analyses, and the marriage of analysis and practice was never fully realized.

However, a present-day submerged-repeater transoceanic cable is a delicate and expensive transmission system. Reducing the amount of cable deposited by as little as one per cent can result in a substantial saving in the first cost of such a system. Its repair is a costly operation requiring the sustenance of an ocean ship and its crew. Therefore, it is important to lay the cable without wasteful excess and with minimum chances for failure after laying. Further, it is important that repair, if necessary, be as efficient as possible. To accomplish these things, an understanding of the dynamics and kinematics of cable laying and recovery is essential.

The purpose of this paper is to provide some of this understanding in as straightforward a way as possible. To this end concepts and results are stressed in the main part of the paper, mathematical details being given in the appendices. Moreover, we hope to show that the results of the analysis can provide a numerical basis for decision making in many of the laying and recovery operations. Most of these results can be expressed in the form of simple formulas and graphs. Several numerical examples are included to illustrate concretely how the results can be applied in practice.

The general plan of the paper is to proceed from simple to more refined models of the laying and recovery processes. Thus, we discuss first what we have called the *two-dimensional stationary model*. This model is appropriate for laying and recovery on or from a perfectly flat bottom while sailing on a perfectly still sea. As a preliminary to this discussion, we consider in some detail the hydrodynamic behavior of typical deep sea submarine cable. We then take up the effects of the ship motions which are induced by wave action and the effects of a bottom of varying depth. These considerations are followed by a short discussion of the problem of controlling the cable pay-out properly during laying and the associated problem of the accuracy of the present taut wire method of determining ship speed. Finally, we consider the *three-dimensional stationary model* and the effects of ocean cross currents.

II. BASIC ASSUMPTIONS

Our analyses, like most analyses of physical problems, are based on idealizations or mathematical models of the actual physical system. The extent of validity of these models must be ultimately determined by experiment and experience. However we shall try to give the reader an idea of when they are clearly applicable and when they are not.

All of the models we consider contain two basic idealizations, namely,

(1) No bending stiffness in cable, i.e., it is a perfectly flexible string,

(2) The average forward speed of the ship is constant.

Bending effects are caused by locally large curvatures, and are significant mainly where the cable leaves the pay-out sheaves and at the ocean bottom. However, for a cable with a steel strength member, bending even to the small radius of the pay-out sheave typically does not materially reduce the tension required to break the cable. Hence, in these cases we can expect an analysis based on the first idealization to give a reasonable idea of when cable rupture will occur. In laying, ship speeds are normally steady and, with the exception of the fluctuations caused by wave action which we consider later in the paper, the second idealization is reasonable also. In recovery, on the other hand, ship speeds are apt not to be steady, and the second idealization is more tenuous. But because of the very slow speeds usually employed, this idealization may in fact be meaningful in recovery as well.

III. TWO-DIMENSIONAL STATIONARY MODEL

3.1 *General*

Assume that the cable ship is sailing at a constant horizontal velocity, that the cable pay-out or haul-in rate is constant, and that the drag of the water on the cable depends only on the relative velocity between the water and the cable. Further, assume that in a frame of reference translating with the ship the cable configuration is time-independent or stationary. This idealized model of the cable laying or recovery process we call the *two-dimensional stationary model.*

This is the model which has been considered in the previous analytical studies.[1-10] As the early investigators quickly pointed out, when the tension at the bottom of the cable is zero, the cable, according to this model, can lie in a straight line from ship to ocean bottom. During laying, when slack is normally paid out, the zero tension condition actually occurs, and hence this case is of considerable practical importance.

The straight line can in fact be shown to be the *only* solution which can satisfy all the observed boundary conditions. This point is discussed in detail in Appendix A. That the straight line is a possible configuration can be seen from Fig. 1. In the vector diagram the velocity of the water with respect to the cable is resolved into a component V_N normal to the cable and a component V_T tangential to it. Associated with V_N and V_T are normal and tangential water resistance or drag forces D_N and D_T. In the straight line configuration, the cable inclination is such that D_N just balances the normal component of the cable weight forces. The situation is thus analogous to that of a chain sliding on an inclined plane, with the forces D_N corresponding to the normal reaction forces of the plane. Summing forces in the normal direction, we get, therefore,

$$w \cos \alpha = D_N , \tag{1}$$

while the summation in the tangential direction gives for T_s, the tension at the ship,

$$T_s = wL \sin \alpha - D_T L. \tag{2}$$

Here w is the weight per unit length of immersed cable, α is the cable's angle of incidence, D_N and D_T are the normal and tangential drag forces per unit length respectively, and L is the inclined length of the cable. For most submarine cable used currently the force $D_T L$ is negligible and we arrive at

$$T_s \approx wL \sin \alpha = wh, \tag{3}$$

where h is the ocean depth at the cable touchdown point. Hence, during slack laying the cable tension at the ship is very nearly equal to the weight in water of a length of cable equal to the ocean depth.

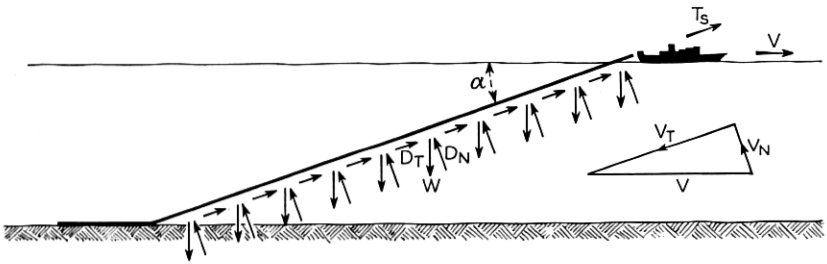

Fig. 1 — Forces acting on a cable in normal laying.

The straight-line solution is the simplest and probably the most important result to be obtained from the stationary two-dimensional model. We shall derive results for other important situations from this model also. As a preliminary, we study first, however, the nature of the normal and tangential drag forces D_N and D_T.

3.2 *Normal Drag Force and the Cable Angle* α

The resistance at sufficiently slow speeds to the flow of a fluid around an immersed body varies as the square of the fluid velocity. This relationship is usually written as*

$$D_N = C_D \frac{\rho V_N^2 d}{2}, \tag{4}$$

* For towed stranded wire experimental verification of this relationship is reported in Reference 11.

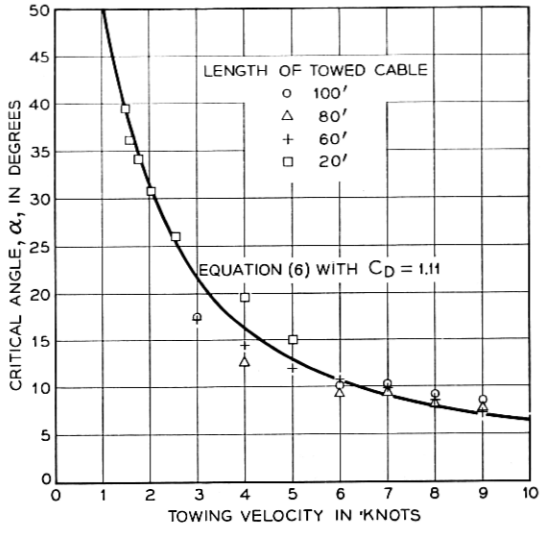

Fig. 2 — Experimental and theoretical variation of critical angle with towing velocity for cable No. 1.

where D_N is the normal drag force per unit length, C_D is the so-called drag coefficient, ρ is the mass density of the fluid, and d is the diameter of the cable. For the straight-line configuration, the vector diagram in Fig. 1 shows that

$$V_N = V \sin \alpha. \tag{5}$$

Substitution of (5) and (4) into (1) yields in turn

$$w \cos \alpha = \frac{C_D \rho V^2 d}{2} \sin^2 \alpha. \tag{6}$$

Equation (6) suggests how the value of the drag coefficient C_D can be obtained experimentally. By towing a length of cable in water at a constant velocity, one can establish the straight-line configuration. The angle α can then be measured as a function of velocity, from which C_D can be computed by (6).

Figs. 2 and 3 show the results of such tests together with plots of (6) for the indicated values of C_D . These results are taken from an analysis by A. G. Norem of experimental data obtained by H. N. Upthegrove, J. J. Gilbert, and P. A. Yeisley. The properties of these cables are listed in Table I.* To eliminate end effects different lengths of cable were towed,

* Cable No. 2 is very similar to present type *D* transatlantic telephone cable. For engineering calculations, type *D* can be considered the same as cable No. 2.

TABLE I — PROPERTIES OF CABLES NO. 1 AND NO. 2

Cable	No. 1	No. 2
Diameter (inches)	0.75	1.25
Wt. in water (lbs/ft.)	0.243	0.705
Outer covering	Polyethylene	Tar impregnated jute
Surface condition	Smooth	Rough
$\overline{EA}$ (twist restrained)	—	4×10^6 lbs
$\overline{EA}$ (twist unrestrained)	—	1.2×10^6 lbs

as is indicated by the plotted experimental points. It is seen that (6) gives a good fit to the experimental data over the entire velocity range.

If the cable has a smooth exterior, an estimate of the drag coefficient C_D can be computed from published values of resistance to flow about an immersed cylinder. This computation is described in Appendix B, where we have also tabulated computed values of C_D. For the smooth cable No. 1, the value of C_D obtained from Appendix B is 1.00 which is in fair agreement with the experimentally determined value of 1.11.

Although the drag coefficient C_D is a fundamental hydrodynamic parameter, it is not the most convenient description of the effect of the nor-

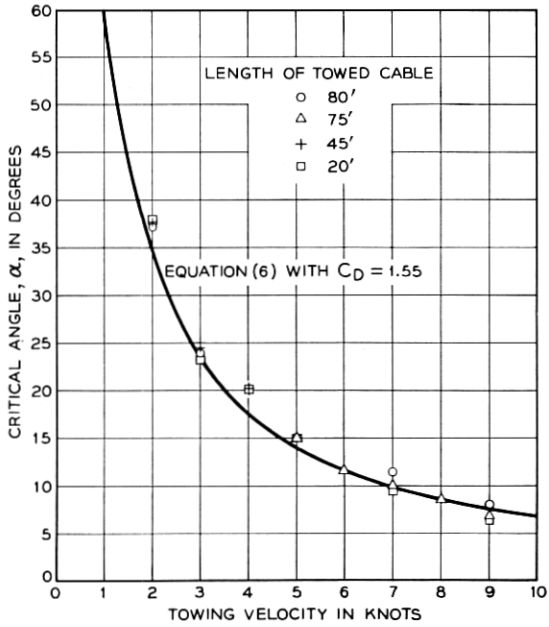

Fig. 3 — Experimental and theoretical variation of critical angle with towing velocity for cable No. 2.

mal component of water velocity. For small values of the incidence angle α

$$\cos \alpha \approx 1,$$

$$\sin \alpha \approx \alpha,$$

and (6) is approximately

$$\alpha_0 V = \left(\frac{2w}{C_D \rho\, d}\right)^{1/2}, \tag{7}$$

where α_0 is the approximate value of α. The quantity $(2w/C_D\rho d)^{\frac{1}{2}}$ is a constant for a given cable. It brings together all the cable parameters which influence the magnitude of the incidence angle α. If the angle α for a given speed is determined accurately, as can be done in a towing test or with a sextant during over-the-stern laying, this quantity is easily computed. Because of its importance, we shall call it the *hydrodynamic constant* of the cable and denote it by H, namely,

$$H = \left(\frac{2w}{C_D \rho\, d}\right)^{1/2}. \tag{8}$$

By virtue of (7) and (8) we may write

$$\alpha_0 V = H. \tag{9}$$

The constant H rather than the drag coefficient C_D will be used from this point on.

When the approximate relationship (9) is not valid, α can be obtained by solving (6). This gives

$$\cos \alpha = \sqrt{1 + \frac{1}{4}\left(\frac{H}{V}\right)^4} - \frac{1}{2}\left(\frac{H}{V}\right)^2, \tag{10}$$

where V is in knots and H in radian-knots. In terms of α_0 we obtain in turn

$$\cos \alpha = \sqrt{1 + \frac{1}{4}\alpha_0^4} - \frac{1}{2}\alpha_0^2. \tag{11}$$

This relationship is shown in Fig. 4, where the incidence angle α is plotted as a function of the approximate incidence angle α_0. It is seen that for $\alpha < 20°$ the difference between α_0 and α is negligible.

Physically α as given by (10) is the angle the cable assumes in the straight-line shape for the velocity V. However, in addition, (10) shows that α can be thought of as a dimensionless parameter which embodies

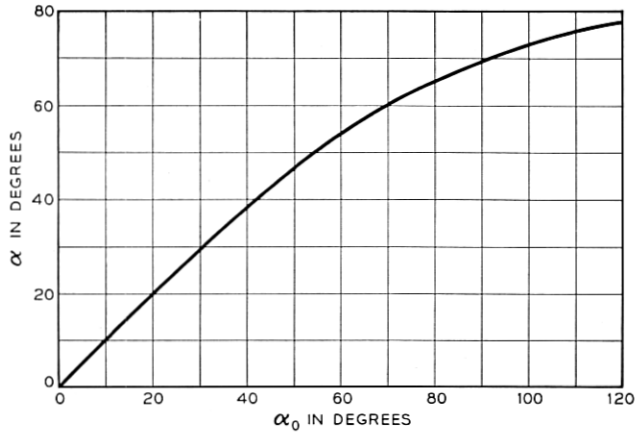

Fig. 4 — Variation of α with α_0 .

both the hydrodynamic properties of the cable and the ship speed. Thus, even when the configuration is not a straight line, we shall find it convenient to express results as a function of the single parameter α, rather than as a function of the two parameters H and V. For this reason, following Pode,[11, 12] we call α the *critical angle*.

3.3 *Tangential Drag Force*

Over the range of velocities encountered in laying and recovery the drag coefficient C_D in equation (6) is essentially constant. However, the corresponding coefficient for the skin friction force associated with V_T, the component of flow along the cable, is not constant. For the cable of smooth exterior (cable No. 1), the expression

$$D_T = C_f \tfrac{1}{2} \rho V_t^2 \pi d, \tag{12}$$

with $C_f = 0.055/(N_R)^{0.14}$, was found to give good agreement with the experimental data, as is shown by Fig. 5. Here D_T is the skin friction or tangential drag force per unit length; V_t is the relative velocity of the water with respect to a cable element given for straight-line laying by

$$V_t = V_c - V \cos \alpha, \tag{13}$$

where V_c is the cable pay-out rate; ρ is the mass density of water; and N_R is the Reynolds number defined as $N_R = V_t L/\nu$, where ν is the kinematic viscosity of water. The data of Fig. 5 are for 100 foot lengths of cable towed in fresh water at a temperature of 60°F.

From (12) we find

$$D_T = \frac{0.055}{2} \rho \frac{\nu^{0.14} V_t^{1.86}}{L^{0.14}} \pi d. \tag{14}$$

This expression indicates that D_T for smooth cable depends on the inclined length of the cable as well as the relative tangential velocity V_t. The form of (13) suggests that the flow tangential to a smooth cable is similar to flow past a smooth plate. In such flow a turbulant boundary layer develops which grows in thickness with distance from the leading edge, resulting in a length dependence of the type shown by (14). Since Fig. 5 refers to 100 foot cable lengths, (13) is probably not accurate for the magnitudes of L occurring in deep-sea laying, and should be used only to obtain the order of magnitude of C_f.

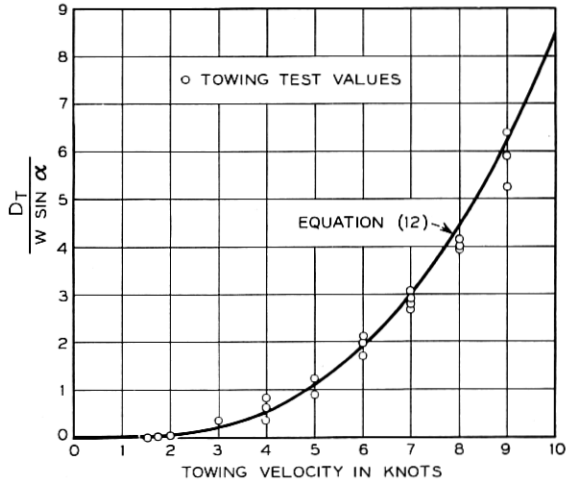

Fig. 5 — Experimental values of the tangential drag force for cable No. 1 compared with those obtained by equation (12).

For the cable with conventional jute outer covering, (cable No. 2), it was found that

$$D_T = 0.01\ V_t^{1.48} \tag{15}$$

fits the experimental data obtained by towing test (Fig. 6). Whereas in (15) the constant 0.055 is dimensionless, the constant 0.01 in this equation has the dimensions necessary to give D_T in units of pounds per foot when V_t is in feet per second. We note that for this cable D_T is independent of the length of the cable.

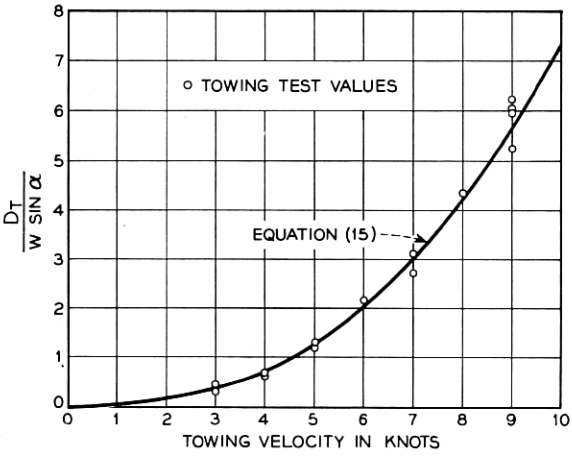

Fig. 6 — Experimental values of the tangential drag force for cable No. 2 compared with those obtained by equation (15).

The ratio of D_T to the tangential component of the cable weight force is given by $D_T/w \sin \alpha$. Equations (14) and (15) indicate that even for small values of α of the order of twelve degrees, $D_T/w \sin \alpha$ is of the order of 6 per cent for relative tangential velocities V_t of 1.0 feet/sec. In many situations V_t will be less than this value, and we can neglect D_T compared to $w \sin \alpha$. As we shall see later, this approximation greatly simplifies the differential equations of the two-dimensional stationary model.

Historically, the question of the variation of D_T with V_t is of some interest. In one of the early papers of 1858 Longridge and Brooks[3] assumed a velocity squared dependence. In 1875, W. Siemens[9] attacked this assumption stating that D_T actually varied linearly with V_t. There ensued a debate in which many bitter words but few experimental data were displayed.[9] In view of our present knowledge that the skin friction force, even in the simplest case of flow past a smooth plate, is the result of complicated boundary layer phenomenon, the existence of this confusion is not surprising.

3.4 *Sinking Velocities and Their Relationship to Drag Forces*

The studies of submarine cable forces in 1857 and 1858 preceded modern fluid mechanics by many years. To characterize the hydrodynamic forces acting on cable the early investigators used *sinking* or *settling* velocities rather than the more recently conceived drag coefficients. The transverse sinking velocity u_s was defined as the terminal velocity attained by a straight, horizontal length of cable sinking in water.

Similarly, the longitudinal sinking velocity v_s was the terminal velocity of a cable length sinking with its axis constrained to be vertical. If for a given cable the drag forces are functions only of velocity, the parameters w, u_s, and v_s, together with the laws of variation of the drag forces with velocity, completely define the hydrodynamic behavior of the cable. Since sinking velocities are still used in submarine cable technology, it is of interest to relate them to the more modern drag coefficient viewpoint.

In the case of transverse or normal flow around the cable, the variation of D_N with the square of the relative transverse velocity gives $(V_N/u_s)^2 = D_N/w$, since at a transverse velocity equal to the sinking velocity the unit transverse drag force is w. Substituting for D_N from (4) we find

$$u_s = \left(\frac{2w}{C_D \rho\, d}\right)^{\frac{1}{2}} = H. \tag{16}$$

Thus, the transverse sinking velocity u_s is identical with the *hydrodynamic consant* H. We can therefore alternatively write the approximate relationship (9) as

$$\alpha_0 V = u_s, \tag{17}$$

where α_0 is in radians and u_s and V are in knots.

For the tangential or skin friction flow along smooth cable, the sinking velocity concept is inadequate because the unit tangential drag force D_T varies with length as well as with the relative tangential velocity V_t. However, for cable with the conventional jute exterior (cable No. 2), we have $(V_t/v_s)^{1.48} = D_T/w$ and from (15) the vertical sinking velocity v_s is $v_s = (46.1w)^{1/1.48}$, where v_s is in knots.

We note in passing that the cable does not, as is sometimes supposed, sink vertically to the bottom at the transverse sinking velocity u_s. Actually, the term "vertical cable sinking rate" is ambiguous. There are in fact two vertical sinking rates which may be important. Although both these rates are normally approximately equal to u_s neither is identical to it.

Relative to the earth, the resultant velocity V_R of a cable element has two components: a horizontal component of the magnitude of the ship velocity, and a component inclined at the angle α of the magnitude of the cable pay-out rate V_c. These are shown in Fig. 7. The component V_{vert} of V_R, given by $V_{\text{vert}} = V_c \sin \alpha$, is the rate at which a cable *element* sinks vertically. For a laying depth h, the time τ it takes for a cable element to sink to bottom is therefore $\tau = h/V_c \sin \alpha$. This time would, for example, tell one how long it takes a lightweight repeater, integral with the cable, to reach the ocean bottom.

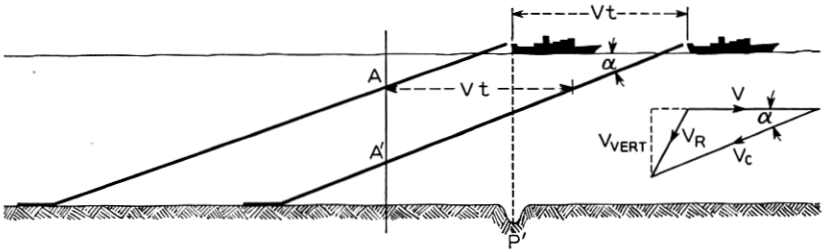

Fig. 7 — Illustration of vertical cable sinking rates.

On the other hand, consider the intersection of the cable *configuration* with a vertical line (Fig. 7). In the time t, as the ship sails a distance Vt, the intersection moves from A to A', a distance $Vt \tan \alpha$. Hence the cable configuration in this sense sinks vertically at the rate $V \tan \alpha$, and the time θ for the configuration to reach bottom in a depth h is $\theta = h/V \tan \alpha$. One may be interested in how long it takes after the ship has passed over an ocean bottom anomaly P' (Fig. 7) for the cable configuration to reach the anomaly. This is just the time θ.

Hence, the vertical sinking rates $V_c \sin \alpha$ and $V \tan \alpha$ can both be of interest. At the usual ship speeds, $\sin \alpha \approx \tan \alpha \approx \alpha \approx u_s/V$. Further V_c normally differs little from V. Hence, both these rates are indeed normally approximately equal to u_s.

3.5 *General Solution of the Stationary Two-Dimensional Model*

Assume that each cable element is traveling along the stationary cable configuration with the constant speed V_c. Starting at the ocean bottom let s be the arc length along the stationary configuration. We define s to be positive in the direction opposite to the direction of travel of the cable elements. So, as Fig. 8 indicates, in laying, positive s is directed from the ocean bottom toward the ship, while in recovery the situation is reversed. We let θ be the angle between the positive s direction and the direction of the ship velocity.

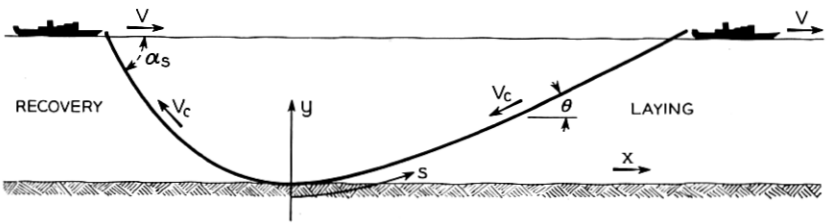

Fig. 8 — Definition of coordinates for the two-dimensional stationary model.

Fig. 9 shows the forces acting on an element of the cable, with tension at the point s being denoted by T. The normal drag force per unit length D_N may, by virtue of (4) and (5), be written in the form

$$D_N = \frac{C_D \rho V^2 d}{2} \sin\theta \mid \sin\theta \mid .$$

It is necessary to introduce here $\mid \sin\theta \mid$ in order for D_N to have the proper sign for all θ. We note, however, that if $V_c \geqq V$, we have from (13)

$$V_t = V_c - V\cos\theta \geqq 0.$$

Hence in normal laying and recovery the unit tangential drag force D_T is always in the positive s direction.

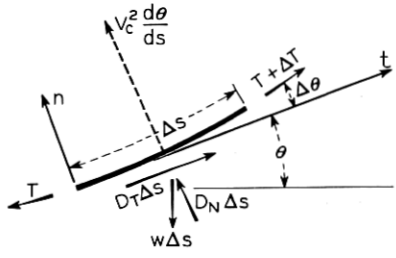

Fig. 9 — Diagram of forces acting on a cable element.

The forces acting on an element produce a centrifugal acceleration $V_c^2 d\theta/ds$. Hence, summing forces along the directions t (tangential) and n (normal), dividing by Δs and sending Δs to zero, we obtain

$$\begin{aligned} &(T - \rho_c V_c^2)\frac{d\theta}{ds} + \frac{C_D \rho V^2 d}{2}\sin\theta \mid \sin\theta \mid - w\cos\theta = 0, \quad \text{(a)} \\ &\frac{dT}{ds} + D_T - w\sin\theta = 0, \quad \text{(b)} \end{aligned} \tag{18}$$

where ρ_c is the mass density per unit length of cable.

It is seen at the outset that $\theta = \alpha$ is a solution of (18a). It is in fact the important straight-line solution which has been discussed in Section 3.1.

If $\theta \neq \alpha$ and D_T varies only with V_t we may divide (18b) into (18a) and integrate to obtain the solution for T in the following form:

$$\begin{aligned} &\ln\frac{(T - \rho_c V_c^2)}{(T_0 - \rho_c V_c^2)} = \int_{\theta_0}^{\theta} \frac{(w\sin\xi - D_T)}{w(\cos\xi - \Lambda\sin\xi \mid \sin\xi \mid)}\, d\xi, \quad \text{(a)} \\ &\Lambda = \frac{C_D \rho\, dV^2}{2w} = \frac{\cos\alpha}{\sin^2\alpha}, \quad \text{(b)} \end{aligned} \tag{19}$$

where T_0 is the tension corresponding to the angle θ_0.

At the cable touchdown point on the ocean bottom only two conditions are possible. If the angle θ is not zero or π there, the cable tension T must be zero. Otherwise a finite tension would act on an infinitesimal length of cable, producing an infinite acceleration. Hence, either the tension T must be zero or the angle θ must be zero or π. The first case normally implies a straight-line configuration (see Appendix A), which has already been discussed. In other cases, we define T_0 as the tension at the touchdown point, and we let θ_0 be zero or π, whichever is appropriate.

If x, y are coordinates in the translating (x, y) frame of a point along the cable configuration, then

$$dx = ds \cos \theta,$$

$$dy = ds \sin \theta.$$

Combining these relations with (18a), we have

$$s = \int_{\theta_0}^{\theta} \frac{(T - \rho_c V_c^2)}{w(\cos \xi - \Lambda \sin \xi \mid \sin \xi \mid)} \, d\xi, \qquad \text{(a)}$$

$$x = \int_{\theta_0}^{\theta} \frac{(T - \rho_c V_c^2) \cos \xi}{w(\cos \xi - \Lambda \sin \xi \mid \sin \xi \mid)} \, d\xi, \qquad \text{(b)} \quad (20)$$

$$y = \int_{\theta_0}^{\theta} \frac{(T - \rho_c V_c^2) \sin \xi}{w(\cos \xi - \Lambda \sin \xi \mid \sin \xi \mid)} \, d\xi. \qquad \text{(c)}$$

Equations (19) and (20) are an integral representation of the complete solution of the basic two-dimensional model. In general, the integrals appearing in these equations cannot be evaluated in terms of elementary functions, and the solution must be obtained by numerical integration. For towing problems where the pay-out velocity is zero, Pode[12] has tabulated these numerical integrations using the approximation that D_T has certain constant values. However, in towing problems the direction of D_T is opposite to what it is in normal laying and recovery problems. Because small magnitudes of D_T were used, these tables nevertheless usually give adequate results in laying and recovery situations as well. At the same time, for submarine cable problems, other approximations allow more convenient ways of evaluating the integrals of (19) and (20).

For example, it is more accurate simply to assume that D_T is zero. As we indicated in Section 3.2, this approximation gives a negligible deviation from the exact solution if the relative tangential velocity V_t is small. Furthermore, in this situation we obtain from (18b)

$$\frac{dT}{ds} = w \sin \theta = w \frac{dy}{ds},$$

and hence the tension at the ship T_s is very nearly

$$T_s = T_0 + wh, \tag{21}$$

where h is the depth at the touchdown point. Thus, if the tangential drag force is negligible, the tension at the ship is essentially the bottom tension plus wh, *regardless* of the nature of the normal drag forces. This is in fact a form of a well-known theorem which, as we shall see in Section 7.1, applies in the three-dimensional case as well.

In the next sections we make further simplifications of the general solution for the specific cases of laying and recovery.

3.6 *Approximate Solution for Cable Laying*

On long cable lays ship speeds are normally of the order of 4–8 knots, with accompanying values of the critical angle α of the order of 10°–30°. For these small values of α, the assumption of zero tangential drag together with some mathematical approximations allow further simplifications of the general solution. These simplifications are derived in detail in Appendix C; here we indicate the results. The angle θ which the configuration makes with horizontal is closely given by

$$\tan\frac{\theta}{2} = \tan\frac{\alpha}{2}\left[\frac{1 - [\overline{T}_0/(\overline{T}_0 + \bar{y})]^{\gamma}}{1 + [\overline{T}_0/(\overline{T}_0 + \bar{y})]^{\gamma}\tan^4\frac{\alpha}{2}}\right]^{1/2}, \tag{22}$$

where $\bar{y}$ and $\overline{T}_0$ are dimensionless depth and bottom tension defined by

$$\bar{y} = y/h,$$

$$\overline{T}_0 = T_0/wh.$$

Here we use the cable angle α in the sense of Section 3.2, namely, as a parameter characterizing the hydrodynamic cable properties and the ship speed. The constant γ is in turn defined by

$$\gamma = \frac{(2 - \sin^2\alpha)}{\sin^2\alpha}. \tag{23}$$

For small α, $\tan^4(\alpha/2)$ is negligible and γ is large. Further

$$0 < \frac{\overline{T}_0}{\overline{T}_0 + y} < 1.$$

Hence, the denominator in (22) is very nearly unity and θ approaches the critical angle α at small values of $\bar{y}$, even for relatively large values of $\overline{T}_0$ of the order of three or four. Thus in the laying case, the cable configuration is very close to a straight line except for a short distance at the ocean bottom.

In Appendix C it is further shown that for small α

$$\begin{aligned} S &= L + \kappa T_0/w, \\ X &= L \cos \alpha + \lambda T_0/w. \end{aligned} \tag{24}$$

Here S and X are the distance along the cable and the horizontal distances respectively from the touchdown point to the ship (Fig. 11), L and $L \cos \alpha$ are the corresponding distances for straight-line laying at the same ship speed, and κ and λ are functions of the critical angle α which are plotted in Fig. 10. To illustrate the use of (24) we consider the following.

Example: Cable No. 2 is being laid without slack onto a rough bottom from a ship moving at six knots. If the pay-out rate is decreased so the slack is 1 per cent negative, what is the subsequent rise of the tension with time at the ship?

This is really a transient problem. However, we shall try to get an idea of the average behavior of the cable by assuming it passes through a sequence of stationary configurations. Also, we assume that because of the rough bottom there is no slippage of the cable along the ocean floor.

If δ is the amount of negative slack and V the ship speed, then in a time t an amount $V(1 - \delta)t$ of cable will have been paid out. This amount plus the inclined length L will equal the amount contained in the curve AOC (Fig. 11). We then have

$$L + V(1 - \delta)t = S + Vt - (X - L \cos \alpha). \tag{25}$$

Substituting (24) into this equation and solving for T_0 we find $T_0 = (w/(\lambda - \kappa))\delta Vt$ and that by (21) the tension at the ship is given by

$$T_s = wh + \frac{w}{\lambda - \kappa} \delta Vt.$$

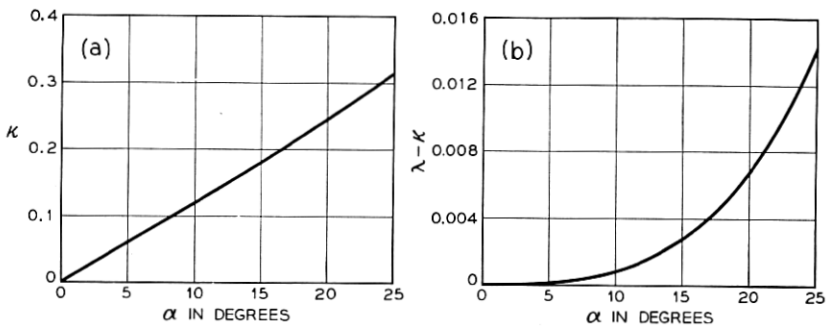

Fig. 10 — Variation of κ and λ with the critical angle.

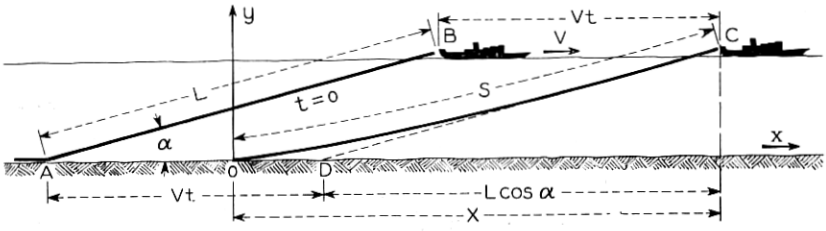

Fig. 11 — Cable geometry at a time t after the onset of negative slack.

For cable No. 2 a ship speed of six knots corresponds to $\alpha = 11.7$ degrees. By Fig. 10, this corresponds to $\lambda - \kappa = 1.4 \times 10^{-3}$. Also $w = 0.705$ lbs/ft by Table I. We get therefore

$$T_s = wh + 3000 \left(\frac{\text{lbs}}{\text{min.}} \right) t.$$

Thus, according to this calculation the tension in this example rises at the extremely rapid rate of 3000 lbs/min. We note also that the rate of tension rise is here independent of the depth h.

In the model which has been postulated, the cable is inextensible; that is, it is assumed not to stretch under load. Because the difference between the lengths of AOC and the sum of the linear segments AD and DC (Fig. 11) is small, one might suspect that the effect of cable extensibility in the present example is important. We can account for this effect in a crude way by assuming that the curve AOC has an additional length corresponding to the stretching caused by the load T_0 acting over the length L. For a cable made of a single material, the stretching would be T_0L/EA, where E is the Young's modulus of the material and A is the cross-sectional area of the cable. In analogy to this we denote the extensile rigidity of the cable by $\overline{EA}$, using the bar to indicate that $\overline{EA}$ is actually a single number obtained directly by measuring the extension of a length of cable loaded in tension. With this notation (25) becomes

$$L + V(1 - \delta)t + \frac{T_0 L}{\overline{EA}} = S + Vt - (X - L \cos \alpha),$$

and repeating the previous computation we find

$$T_s = wh + \frac{w}{\left[\dfrac{wh}{\overline{EA} \sin \alpha} + \lambda - \kappa \right]} V \delta t.$$

It is to be noted that in this computation, unlike the inextensible case, the rate of tension rise depends on the depth h.

For conventional helically armored cable, one cannot define a single extensile rigidity because of coupling between pulling and twisting. Thus, how such a cable extends under tension depends on how it is restrained from twisting at the ship and at the ocean bottom. Instead of trying to determine these end restraints, we consider the limiting cases of no restraint and complete restraint to twisting. Data supplied by P. Yeisley indicate the values of $\overline{EA}$ for cable No. 2 in these conditions to be those given in Table I (Section 3.2). If we take $h = 6{,}000$ and 12,000 feet, we find with these values that

$h = 6000$ feet:

$$T_s = wh + 220 \text{ (lb/min)}t \text{ (twist unrestrained)},$$
$$= wh + 640 \text{ (lb/min)}t \text{ (twist restrained)},$$

$h = 12{,}000$ feet:

$$T_s = wh + 120 \text{ (lb/min)}t \text{ (twist unrestrained)},$$
$$= wh + 360 \text{ (lb/min)}t \text{ (twist restrained)}.$$

Comparing with the inextensible computation, we see that the extensibility markedly reduces the rate of tension build-up. Nevertheless, even for the case of no restraint to twisting at a depth of 12,000 feet the rise rate is a relatively high 120 lb/min. Hence, at least over a rough bottom, the tension would quickly indicate the onset of negative slack, although the sensitivity of this indication would decrease with increasing depth.

3.7 *Approximate Solution for Cable Recovery*

Fig. 8 illustrates how cable is in present practice recovered from the ocean bottom. The cable is in front of the ship as it is brought in over the bow, and the ship pulls itself along the cable. In this process the cable tends to guide or lead the ship directly over its resting place on the ocean bottom.

It is clear that during recovery by this procedure the tension at the ocean bottom is not zero and the cable configuration is not a straight line. Furthermore, in this situation the normal component of the water drag force D_N pushes down on the cable instead of buoying it up as in the case of laying. This in turn implies a higher tension at the ship during recovery than during laying.

If the tangential drag is neglected, the tension at the ship T_s during recovery is given in dimensionless form by (see Appendix C)

$$\frac{\overline{T}_s - 1}{\overline{T}_s} = \left[\tan^2 \alpha \, \frac{\cos \alpha + \cos \alpha_s}{1 - \cos \alpha \cos \alpha_s}\right]^{1/\gamma}, \tag{26}$$

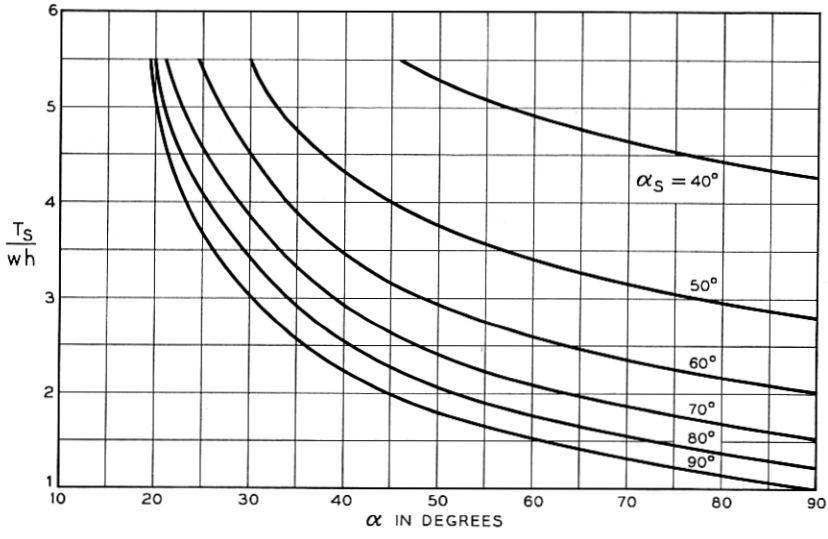

Fig. 12 — Variation of the tension factor for recovery with the critical angle α.

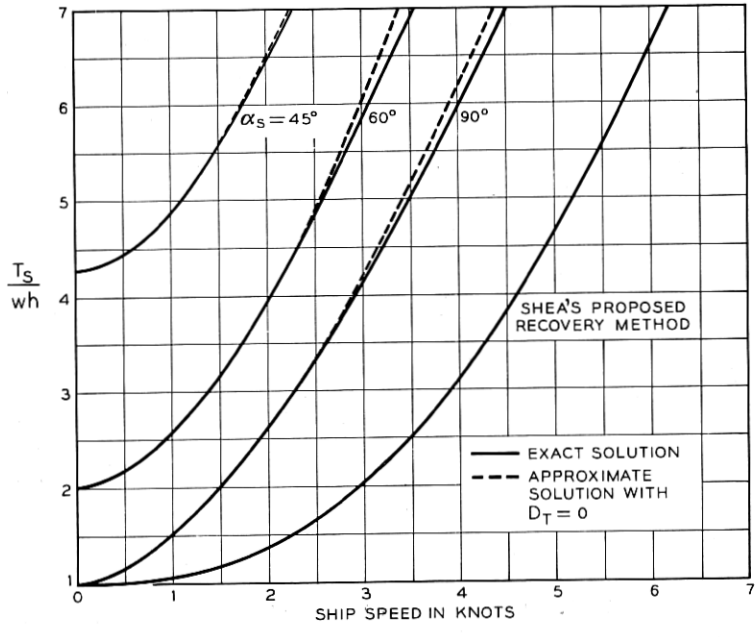

Fig. 13 — Variation of exact and approximate tension factors for recovery of cable No. 2.

where $\overline{T}_s$ is the tension factor defined by $\overline{T}_s = T_s/wh$ and γ is given by (23). Equation (26) is plotted in Fig. 12 in the form of $\overline{T}_s$ versus α for various surface incidence angles α_s (Fig. 8). It is seen that the recovery tensions are in fact considerably higher than the laying tension of approximately wh.

To illustrate the smallness of the error of neglecting the tangential drag force in this computation, we have plotted the approximate and exact curves of $\overline{T}_s$ versus ship velocity for cable No. 2 in Fig. 13. The dotted curves have been computed from (26), while the solid curves have been obtained by substituting D_T from (15) into (19) of the general solution and integrating numerically.* (The curve labeled Shea's recovery method is discussed in the next section.)

The distance along the cable S and the horizontal distance X from the touchdown point to the ship cannot be expressed in a simple form as in the case of laying. However, they can be obtained by numerical integration from (20). The results of this computation for $D_T = 0$ are shown in Figs. 14 and 15.

How Figs. 12, 14 and 15 can be used is illustrated in the following example.

* The standard form of Simpson's rule was used for all the numerical integrations mentioned in the paper. In each case the interval of integration was chosen fine enough to obtain at least three significant figure accuracy.

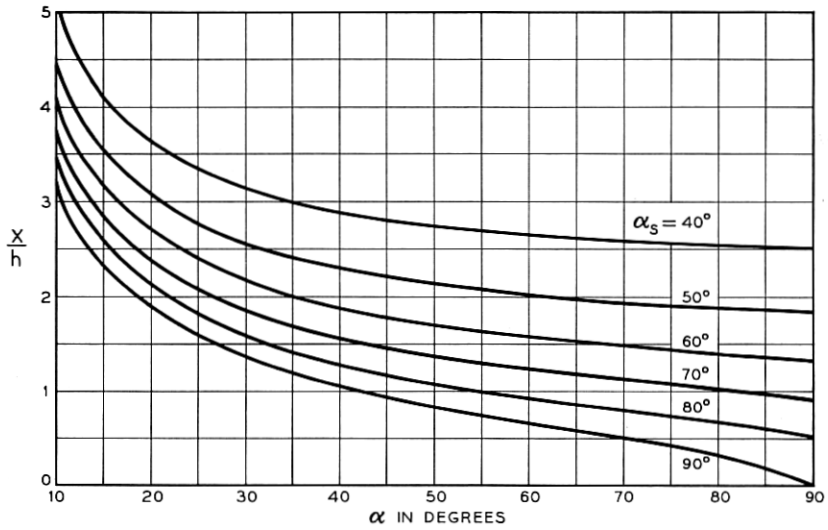

Fig. 14 — Variation of the horizontal distance to the touchdown point during recovery with the critical angle.

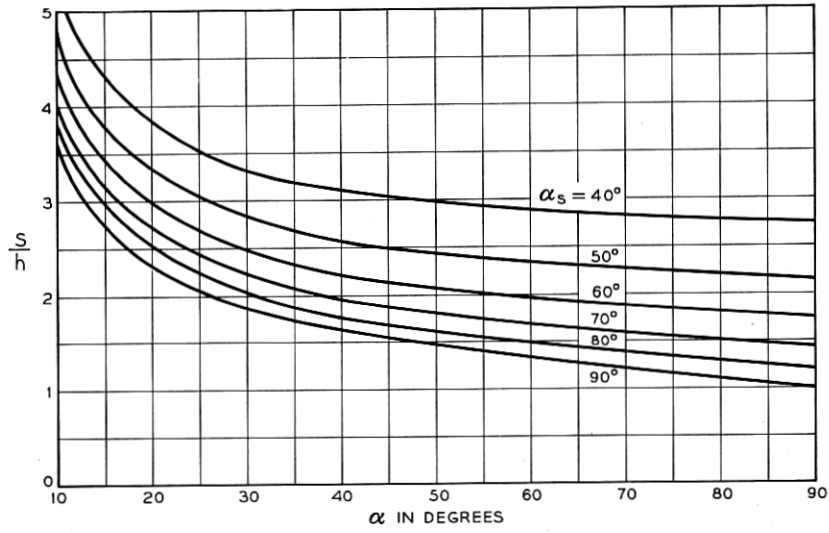

Fig. 15 — Variation of the distance along the cable to the touchdown point during recovery with the critical angle α.

Example: A cable weighing 0.7 lb/ft in sea water and having a hydrodynamic constant H of 70 degree-knots, is to be picked up from a depth of two thousand fathoms. If the ship speed is one knot what is the cable tension at the ship for surface angles α_s of 40°, 60°, and 90°? How far in front of the ship and how far along the cable will the touchdown point be for these values of α_s ?

As indicated by (9), an H value of 70 degree-knots together with a ship velocity of one knot yields $\alpha_0 = 70$ degrees. Fig. 4 yields in turn $\alpha = 60$ degrees. Entering Fig. 12 with this value of α, we can obtain T_s/wh. In this example the wh tension for a depth of two thousand fathoms is 8,400 lb, and hence the values of T_s/wh and $\overline{T}_s$ are as follows:

α_s	T_s/wh	T_s
40°	4.85	40,700 lbs
60°	2.58	21,700 lbs
90°	1.53	12,900 lbs

From Fig. 14 we get in turn for the horizontal distance from the ship to the touchdown point

α_s	X/h	X
40°	2.65	5300 fathoms
60°	1.56	3120 fathoms
90°	0.66	1320 fathoms

Finally, from Fig. 15 we get for the distance along the cable to the touchdown point

α_s	S/h	S
40°	2.88	5760 fathoms
60°	1.95	3900 fathoms
90°	1.33	2660 fathoms

3.8 *Shea's Alternative Recovery Procedure*

The high tensions which result in the usual recovery operation require slow ship speeds of the order of one knot or less if the cable is not to be broken. One wonders if it is possible to mitigate these tensions and thus speed the recovery process. J. F. Shea discovered that this can theoretically be done by allowing α_s to exceed 90°, thus establishing the straightline configuration (Fig. 16). As in laying, the normal drag forces in this scheme support the cable, rather than push down on it as in conventional recovery. However, in contrast to the laying situation we have $V_t = V_c + V \cos \alpha$. Thus V_t is the sum of V_c and $V \cos \alpha$ instead of their difference and D_T is not necessarily negligible. Furthermore, the direction of D_T is now such as to increase rather than decrease the tension over the wh value. Hence, instead of (2), a summation of forces along the cable yields $T_s = wh + D_T L$, and the tension at the ship can be considerably higher than wh. A curve of T_s as a function of ship speed for cable No. 2 is shown in Fig. 13 with the label "Shea's recovery method". This has been computed for the case of haul-in speed equal to ship speed by means of the above equation and (15). It is seen that the tensions computed for this method of recovery, at least for the cable No. 2, are nevertheless considerably smaller than those which occur in the usual recovery procedure. It would seem that the straight-line recovery technique could fruitfully bear further examination, especially for application to the recovery of long stretches of cable.

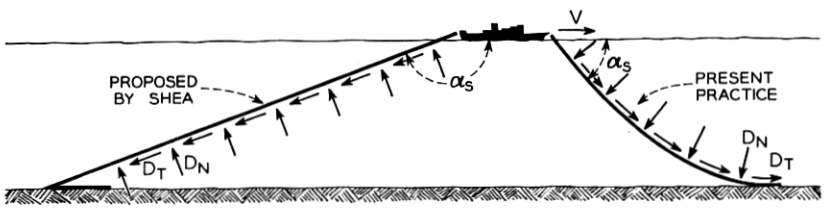

Fig. 16 — The present and Shea recovery methods.

IV. EFFECTS OF SHIP MOTIONS

4.1 *Tensions Caused by Ship Motions*

In the basic stationary model a perfectly calm sea is postulated. However, in reality, wave action gives rise to a random motion of the ship which in turn induces variations in cable tensions around those corresponding to the basic model.

To analyze this effect, we assume that the mean forward velocity of the ship and the mean pay-out or haul-in rate are constant and that the mean tension at the ship and the mean direction of the cable as it enters water are those given by the stationary model. In a reference frame moving with the mean velocity, we resolve the ship displacement into a longitudinal component P_0 (Fig. 17) along the mean or stationary direction and a transverse component Q_0 perpendicular to the stationary direction.

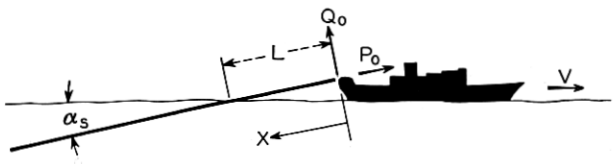

Fig. 17 — Longitudinal and transverse components P_0 and Q_0 of the ship displacement.

Intuitively, one might expect the tensions caused by the transverse displacement Q_0 to be negligible compared to those caused by the longitudinal displacement P_0. An analysis we have carried through in fact yields this conclusion. Because of its complexity and length, this analysis and the model upon which it is based are given in Appendix D. The results for the case of harmonic variation of Q_0 with time indicate, at least for cable No. 2, that the tension associated with the transverse component Q_0 is indeed negligible for all except ship motions so extreme as to rarely occur.

In addition, this analysis indicates that for the transverse disturbance Q_0, the amplitude of the responding transverse cable motion decreases exponentially after the cable enters the water because of the damping action of the water drag forces. The "half-life" distance for cable No. 2, that is, the distance along the cable at which the amplitude of a harmonic transverse motion is damped to one-half its surface value, is plotted in Fig. 18 as a function of the period of the motion for various depths h and ship velocities V. The striking feature of these figures is the rapidity of this damping. The analysis thus shows for cable No. 2 that the eflect of a transverse disturbance penetrates only a short distance into the water.

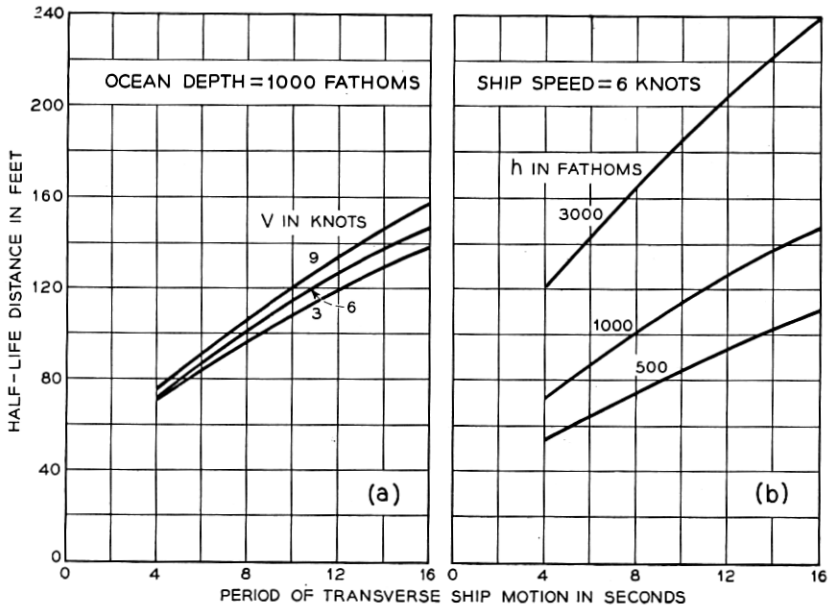

Fig. 18 — Variation of half-life distance of cable No. 2 with the period of ship motion.

As far as cable tensions are concerned, the important ship displacement then is the longitudinal component P_0, directed along the stationary direction of the cable. The analysis of Appendix D leads to the basic one-dimensional wave equation

$$\frac{\partial^2 p}{\partial x^2} - \frac{1}{c_1^2}\frac{\partial^2 p}{\partial t^2} = 0 \tag{27}$$

for the description of the longitudinal motion. In this equation p is the deviation in longitudinal displacement from the mean pay-out or haul-in displacement, and the remaining symbols are defined as (Fig. 17)

x = distance from the mean ship position along the stationary cable configuration,
t = time,
$c_1^2 = \overline{EA}/\rho_c$.

The additional tension T_p due to ship motion is in turn given by

$$T_p = \overline{EA}\frac{\partial p}{\partial x}. \tag{28}$$

As in the example of Section 3.6, we have again assumed that by using

in (28) the limiting values of $\overline{EA}$ obtained by complete restraint to twisting and no restraint to twisting during pulling, one can obtain bounds on the actual displacements and tensions.

The solution of (27) under arbitrary boundary conditions can be obtained from standard textbooks. Probably it is most representative to assume the cable is semi-infinite. That is, although damping of the cable is normally so small that we neglect it in (27), we may assume, because of the cable's great length, that the damping is sufficient to cause complete decay of a disturbance initiated at the ship, and that such a disturbance is not reflected from the ocean bottom. Under this condition the additional tension T_p is given by

$$T_p = -\sqrt{\overline{EA}\rho_c}\,\frac{dP}{dt}, \tag{29}$$

where $P = P_0 + P_1$ with dP_1/dt being in turn the increment in pay-out rate or decrement in haul-in rate from the mean. For cable No. 2, Table I (Section 3.2) indicates that

$$\sqrt{\overline{EA}\rho_c} = 220 \text{ lb/ft/sec (twist unrestrained)},$$
$$= 400 \text{ lb/ft/sec (twist restrained)}.$$

Two examples will make clear the application of (29).

Example 1: Steady-State Laying or Recovery in a Regular Seaway.

Assume that in a frame of reference traveling at the mean horizontal ship velocity ship surging (to and fro forward motion) is zero and the combined heave and pitch motion is normal to the ocean surface and is given by

$$W = A \sin 2\pi \frac{t}{\tau}.$$

If the period τ is 6 seconds and the amplitude A is 15 feet find for cable No. 2,

a) $(T_p)_{\max}$ for laying at a constant pay-out rate and at a ship speed of 6 knots,
b) $(T_p)_{\max}$ for recovery at a constant haul-in rate and with a surface incidence angle of 60°.

In both cases (a) and (b), the deviation P_1 in pay-out or haul-in rate is zero, hence $P = P_0 = W \sin \alpha_s$, and $(dP/dt)_{\max} = (2\pi/\tau)\, A \sin \alpha_s$. Since

cable No. 2 has a hydrodynamic constant H of 70 degree-knots, we have in case (a)

$$\alpha_s = 11.7 \text{ degrees and } \left(\frac{dP}{dt}\right)_{\max} = 2.12 \text{ ft/sec.}$$

From (29) we get therefore

$$(T_p)_{\max} = 466 \text{ lbs (twist unrestrained),}$$
$$= 848 \text{ lbs (twist restrained).}$$

In case (b) we have $\alpha_s = 60°$, $(dP/dt)_{\max} = 13.6$ ft/sec, and hence

$$(T_p)_{\max} = 2{,}990 \text{ lbs (twist unrestrained),}$$
$$= 5{,}430 \text{ lbs (twist restrained).}$$

During recovery by conventional methods the surface incidence angle α_s is in general much larger than that which occurs during laying. The above example points up that one can expect correspondingly larger ship motion tensions during recovery than during laying in the same sort of seas. Since the stationary tensions are also much larger during recovery, recovery is the condition for which the strength of the cable should be designed.

In this example we have considered a regular seaway, something which does not exist in nature. Recent work in the application of the theory of stochastic processes to the study of ocean waves and ship dynamics promises to develop into a realistic description of the behavior of ships at sea.[13] When such a description becomes available, we shall be able to obtain a better estimate of the magnitudes of ship motion tensions.

As far as data presently available are concerned, the maximum storm condition vertical velocity at the bow or stern recorded by the *U.S.S. San Francisco* during her research voyage of 1934 was 22 feet/sec.[14] Since this ship was roughly the size of a cable ship such as the *H.M.S. Monarch*, this figure might indicate the order of the maximum velocities to be expected in cable practice. In terms of our example, for six knot laying this vertical velocity would imply

$$T_p = 980 \text{ lbs (twist unrestrained),}$$
$$= 1{,}780 \text{ lbs (twist restrained).}$$

For recovery at a surface incidence angle of 60°, it would imply in turn

$$T_p = 4{,}200 \text{ lb (twist unrestrained),}$$
$$= 7{,}600 \text{ lb (twist restrained).}$$

However, it is to be cautioned that these numbers are merely indicative and might differ considerably from those which occur on a particular cable ship.

Example 2: Brake Seizure

While laying cable No. 2 at six knots in a perfectly calm sea, a sudden seizure of the brake occurs. What is the resulting initial rise in tension?

Because of the calm sea we have $P_0 = 0$. Therefore

$$\frac{dP}{dt} = P_1 = -V \cos \alpha_s .$$

With the value of $V = 6$ knots and a corresponding α_s of 11.7° (see Example 1) we have $dP/dt = 9.9$ ft/sec and hence from (29)

$$T_p = 2180 \text{ lbs (twist unrestrained)},$$

$$= 3970 \text{ lbs (twist restrained)}.$$

These values of T_p pertain only to the transient values occurring while the tension wave is being transmitted to the ocean bottom. If the seizure in this case occurred at a depth of three thousand fathoms, the time of transit to the ocean bottom would be only of the order of nine seconds. After reaching bottom our initial assumption of no reflection from the bottom would be violated and (29) would no longer hold. In reality the cable tension would continually increase at the ship and reversing ship engines or some other action would be required to avoid rupture of the cable.

V. DEVIATIONS FROM A HORIZONTAL BOTTOM

5.1 *Kinematics of Laying Over a Bottom of Varying Depth*

Ocean bottom topography is not everywhere flat and horizontal as postulated in the basic model. In the Mid-Atlantic ridge, for example, there exist bottom slopes of thirty or forty degrees. In other places submarine canyons with almost vertical sides have been found. Furthermore, where the bottom is steepest it is most likely to be rocky and craggy since erosion tends to smooth out a sandy or muddy bottom. Therefore, it is important to know how the cable should be paid out to cover a bottom of varying depth. To help determine this, we extend here the stationary model to the case of a non-horizontal bottom.

In Section 3.1 we indicated that if the cable tension at the touchdown point is zero the configuration according to the basic model is a straight line, regardless of how the cable is paid out. If the cable is paid out with

slack with respect to the bottom, the zero touchdown tension condition is fulfilled. Hence, under the proper slack pay-out, the cable geometry and, as we shall see, the cable kinematics are particularly simple.

Essentially, we must consider two deviations from the horizontal bottom, namely, downhill or descent laying and uphill or ascent laying. We consider these situations in turn, confining ourselves to bottoms of constant slope since any bottom contour can be approximated by straight-line segments.

To cover a descending bottom, the cable pay-out rate must exceed the ship speed, Fig. 19(a). To cover an ascending bottom, the angle of incidence α of the cable, which as we have seen in Sections 3.1 and 3.2 depends only on the ship speed, must exceed the ascent angle γ, Fig. 19(b). Otherwise, the situation shown in Fig. 19(c) develops. Hence the critical parameters are pay-out speed and ship speed.

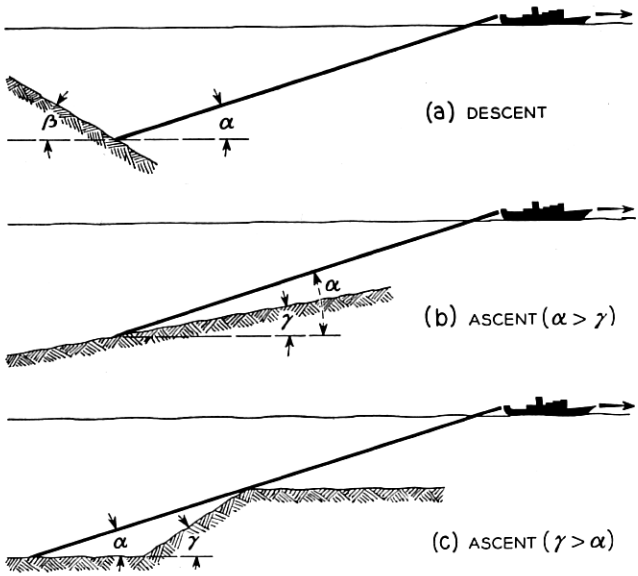

Fig. 19 — Cable geometry during straight-line descent and ascent laying.

During descent laying we see from Fig. 20 that in a time t an amount of cable equal to $a + b$ must be paid out. Hence the required pay-out rate V_c is $(a + b)/t$. But by straightforward trigonometry

$$V_c = \frac{a + b}{t} = \frac{\sin \alpha + \sin \beta}{\sin (\alpha + \beta)} V, \tag{30}$$

where β is the angle of descent and α is the straight-line incidence angle.

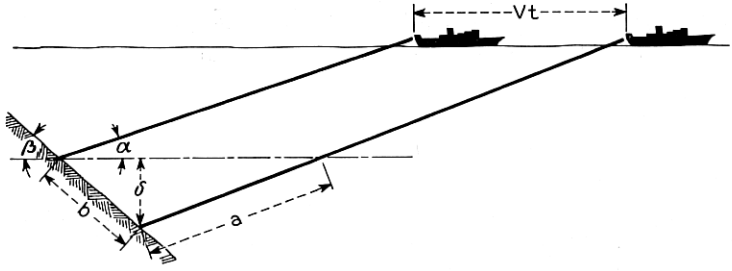

Fig. 20 — Kinematics of straight-line descent laying.

In accordance with usual terminology we define the *slack* ϵ as

$$\epsilon = (V_c - V)/V. \tag{31}$$

We shall think of the slack as being composed of two parts: a *fill* f, which is the amount of slack required for the cable to cover the bottom, and an *excess*, equal to $\epsilon - f$, which will normally be laid to provide a margin of safety. Substituting V_c from (31) into (30) we get the expression for the fill f. The result can be transformed to the form

$$\tan \frac{\alpha}{2} \tan \frac{\beta}{2} = \frac{f}{2 + f}. \tag{32}$$

The quantities α, β and f are normally all small quantities and we may make the approximations

$$\tan \frac{\alpha}{2} \approx \frac{\alpha}{2},$$

$$\tan \frac{\beta}{2} \approx \frac{\beta}{2},$$

$$\frac{f}{2 + f} \approx \frac{f}{2}.$$

For α, $\beta < 30°$ and $f < 0.06$, the error in each of these approximations is less than 3 per cent. Hence, with good accuracy we write (32) as

$$f = \frac{\alpha\beta}{2}, \tag{33}$$

where α and β are expressed in radians. Further, we have from (9) that α in radians is very nearly $\alpha = H/V$, where H is in radian knots. Substituting this expression into (33), we get for the fill

$$f = \frac{H\beta}{2V} . \tag{34}$$

Finally, using this expression for f in (31), we arrive at*

$$V_c - V = \frac{H\beta}{2}. \tag{35}$$

Thus, the *increment* in required pay-out rate is essentially a function only of the descent angle β and is *independent* of ship speed.

In the case of an ascending bottom for which $\alpha > \gamma$, Fig. 19(b), positive bottom slack may be obtained with a pay-out of less than the ship speed. The allowable decrement in pay-out rate is given by

$$V - V_c = \frac{H\gamma}{2}, \tag{36}$$

that is, the same as the required increment for ascent laying. Likewise, the fill f in this case is simply $f = -(H\gamma/2V)$.

The only way to avoid the situation shown in Fig. 19(c) where $\alpha < \gamma$ is to sail slowly enough to maintain an incidence angle α greater than the angle of rise γ. By (9), we have for most laying speeds $\alpha V \approx H$. With good accuracy the condition $\alpha > \gamma$ thus implies

$$V < \frac{H}{\gamma}. \tag{37}$$

Therefore, for a given rise γ the limiting ship speed is simply H/γ.

5.2 *Time-Wise Variation of the Mean Tension in Laying Over a Bottom of Varying Depth*

In the cases where the cable is paid out with excess onto a bottom of constant slope, the variation of the mean tension at the ship with time is easily computed. During descent laying the increase in depth δ after a time t is by elementary trigonometry (Fig. 20)

$$\delta = \frac{\sin\alpha \sin\beta}{\sin(\alpha + \beta)} Vt.$$

Hence, the rate of rise of the mean shipboard tension is

$$\frac{dT}{dt} = \frac{w\delta}{t} = \frac{\sin\alpha \sin\beta}{\sin(\alpha + \beta)} wV. \tag{38}$$

Similarly, during an ascent lay for which the bottom is less steeply

* Note that in (33), (34) and (35), H may be replaced by the numerically identical transverse settling velocity u_s (see Section 3.4).

inclined than the cable ($\alpha > \gamma$), the rate of decrease in shipboard tension is

$$\frac{dT}{dt} = -\frac{\sin \alpha \sin \gamma}{\sin (\alpha - \gamma)} wV.$$

Like negative slack laying on a flat bottom, the variation of tension with time depends greatly on the frictional characteristics of the bottom in cases other than the above. We therefore limit ourselves to situations where the cable does not move with respect to the ocean floor. This case might be approximated by rough bottoms, where the cable might wedge itself between rocks.

A nomograph giving a rough estimate of the rise of mean tension with time when a cable becomes completely suspended is worked out in Appendix E. In deriving this nomograph it is assumed that the cable takes on a sequence of stationary configurations. This assumption is probably reasonable if the time span of the tension rise is large compared to the time of passage of a tension wave from the ship to ocean floor and return, which as mentioned in Section 4.1 is of the order of 18 seconds. However, because of this assumption and others mentioned in Appendix E, we regard the tension variation computed by the nomograph only as a crude approximation.

Fig. 21 shows the mean ship-board tension versus time computed by means of the nomograph for various slacks ϵ, where ϵ is defined by (31). The values which were used for the other parameters entering the calculation were

$$\frac{wh}{EA} = 3.1 \times 10^{-3},$$

$$\alpha = 12°.$$

Also shown on this curve is the tension rise computed for the case of laying down a vertical slope without excess. The rise for this case is given by (38) with $\beta = 90°$. It is seen that as the slack ϵ is increased the curves for a complete suspension approach the $\beta = 90°$ curve. Indeed, it can be shown that under the assumptions made in computing Fig. 21 the $\beta = 90°$ curve gives a lower bound on the tension rise with time in the case of a complete suspension. A tension rise rate greater than the $\beta = 90°$ rate is thus an indication of unsatisfactory covering of the bottom.

In the case of too rapid a ship speed resulting in $\alpha < \gamma$ (Fig. 19c) restraint of movement of the cable along a rough bottom would cause the tension on the high side of the crest to be zero. There would thus be a sudden drop in tension corresponding to the sudden decrease in depth at the touchdown point after the cable was laid over the crest of the hill.

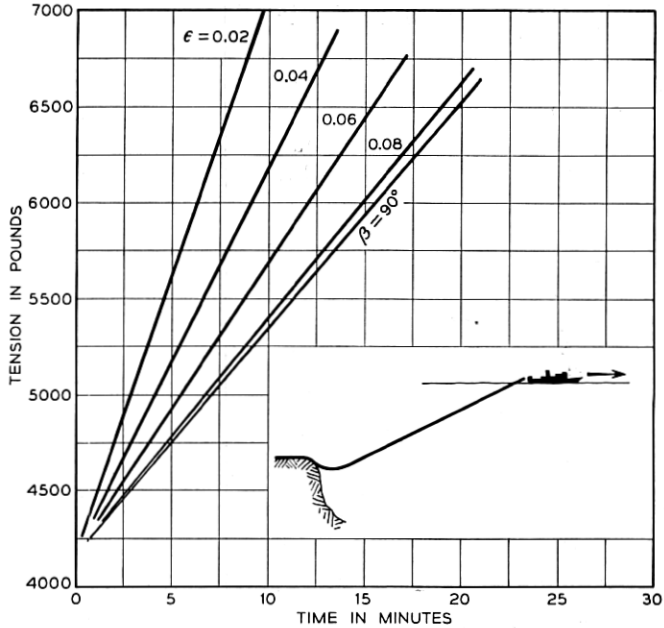

Fig. 21 — Variation of tension with time when cable No. 2 is completely suspended.

On the other hand, in the case of a frictionless bottom, the removal of the supporting water drag forces would cause the cable to seek a catenary equilibrium position on the low side of the crest. But in doing this, the cable would drag itself over the crest, with an accompanying *increase* in shipboard tension.

Thus for the case of a bottom rise steeper than the cable inclination ($\alpha < \gamma$) either an increase or a decrease of tension with time is possible, depending on the nature of the bottom.

5.3 *Residual Suspensions*

If the cable is not paid out rapidly enough, or if the ship speed is excessive, the cable will be left with residual suspensions after it has been laid. To get an idea of the possible magnitudes of the tensions accompanying these suspensions, we consider here some numerical examples pertaining to cable No. 2. As before, we assume for definiteness the extreme case of a bottom rough enough to prevent movement of the cable.

In Fig. 22 is shown the profile of a 35 fathom (210 feet) increase in depth with a maximum slope of 45°. This profile was obtained from

fathometer records of the Mid-Atlantic Ridge provided by Professor Bruce C. Heezen of the Lamont Geological Observatory. Laying down this slope at a ship speed of six knots requires a slack of 8.5 per cent (see Section 5.1). If the slack were only 5 per cent, the successive cable configurations as calculated by the methods of Appendix E would be those shown in Fig. 22(a).* The cable would touch bottom after 2.6 minutes,

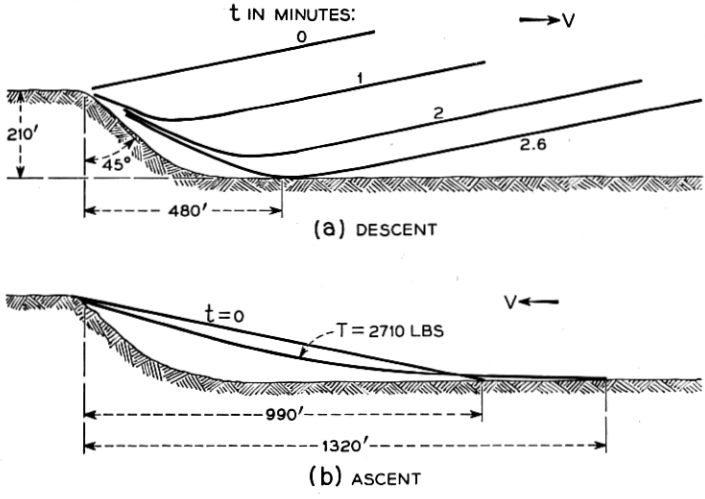

Fig. 22 — Successive cable configurations during a 35-fathom descent and ascent lay of cable No. 2 at a 6,000-ft depth with an assumed 5 per cent slack and 6-knot ship speed.

leaving a residual suspension with a half-span of 480 feet and a tension of 525 lbs. The mean tension at the ship would correspondingly increase by 525 lbs during the 2.6 minute time interval. In even moderately rough seas, this tension change could be obscured by the ship motion tensions.

Consider this profile next to represent an ascending lay under a ship speed of six knots. Fig. 22(b) shows the initial ($t = 0$) and residual cable configuration. Because of the small incidence angle of the initial straight-line shape, the residual half-span of the catenary is a quarter of a mile (1320 feet) long, and the accompanying residual tension is 2,710 lbs, or roughly that which normally occurs in laying at a depth of $\frac{3}{4}$ of a nautical mile. At the ship, there would be a decrease in the mean tension of 130 lbs. corresponding to the 35 fathom decrease in depth. Again, a tension change of this magnitude would be difficult to discern because of ship motion tensions.

* We have further taken the ratio $wh/\sqrt{EA}$ to be 3.1×10^{-3} in this computation. However, the results are very insensitive to change in the $wh/\sqrt{EA}$ ratio.

If the above 35 fathom change occurred at a depth of say three thousand fathoms, a very sensitive fathometer would be required to detect it. Thus, although complete restraint of cable movement along the bottom is an extreme and unlikely condition, the above examples indicate that long residual suspensions can occur with essentially no manifestation at the ship, especially in deep water.

VI. CABLE LAYING CONTROL

6.1 *General*

We have seen that the mean cable tension at the ship reflects the amount of slack which is being paid out and how the cable is covering the bottom. However, in most cases this reflection is not sensitive. For example, the tangential drag force D_T varies with V_t, the longitudinal velocity of the cable relative to the water. In theory, as (2) shows, one can therefore determine the amount of slack being paid out from shipboard tension measurements. For cable No. 2, we have plotted in Fig. 23 the variation of the mean tension at the ship as a function of slack for a ship speed of six knots and a depth of two thousand fathoms. At three per cent slack the tension is 8,240 pounds, while at six per cent slack it is 8,020 pounds, a difference of only 220 pounds. This amount of tension

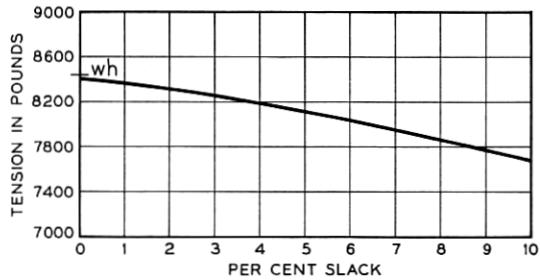

Fig. 23 — Variation of shipboard tension with per cent slack for laying cable No. 2 at a ship speed of 6-knots in a depth of two thousand fathoms.

could be easily obscured by the effect of ship motion. Thus, to measure slack accurately by relating it to cable tensions one would have to know the depth and cable parameters very precisely and, in addition, would need a very efficient filter to separate out the "noise" tension caused by ship motion.

Similarly, it has been shown that residual suspensions can occur with essentially no reflection in the tension readings at the ship. Hence, although tension readings can give a valuable check on how the cable is

covering the bottom, it would seem difficult for them to provide exact enough data for the control of cable laying.

At the same time we have seen that if the bottom contour is known in advance, then for a given ship speed one can compute the required cable pay-out rate. Also with foreknowledge of the bottom, one can anticipate steep bottom ascents and decrease the ship speed accordingly. Such a purely kinematic attack on the cable laying problem would seem more fruitful than an attack which depends on measurements of shipboard cable tensions.

Possibly the simplest way of measuring the bottom contour is by means of a fathometer located at the ship. Since the cable ship is normally far forward of the touchdown point of the cable, one could in theory obtain in this manner the required advance knowledge of the contour. In present practice, a taut piano wire is used to obtain the ground speed of the ship. We examine briefly the accuracy of this method in the next section.

6.2 *Accuracy of the Piano Wire Technique*

The taut wire is laid simultaneously with the cable, but under a constant mean shipboard tension. If the bottom is perfectly horizontal, the speed of the wire coincides with the ground speed of the ship. However, when the bottom depth is variable and the wire is laid up and down hill, the wire's pay-out speed deviates from the ship speed. By (31), it is seen that the error in the ship speed which is indicated by the wire is just equal to the slack ϵ with which the wire is paid out. This slack, which may be positive or negative, can in turn be estimated by the methods of the previous sections.

Consider the beginning (denoted by (1) in Fig. 24) and end (denoted by (2) in Fig. 24) of a downhill lay of the piano wire. As before we neglect the tangential drag force. Then, the condition that the tension at the ship remains constant gives, by (21),

$$(T_0)_1 + wh_1 = (T_0)_2 + wh_2 , \tag{39}$$

where the subscripts 1 and 2 refer to the configurations at the beginning and end of the downhill lay. If $\bar{\epsilon}$ is the average slack or error of the piano wire during the descent, then $(1 + \bar{\epsilon})V$ is its average pay-out rate, and we have by Fig. 24,

$$S_1 + (1 + \bar{\epsilon})Vt = \frac{h_2 - h_1}{\sin \beta} + S_2 , \tag{40}$$

where S_1 and S_2 are lengths along the cable from the touchdown point to the ship. Also, from Fig. 24

$$X_1 + Vt = (h_2 - h_1)/\tan \beta + X_2 . \tag{41}$$

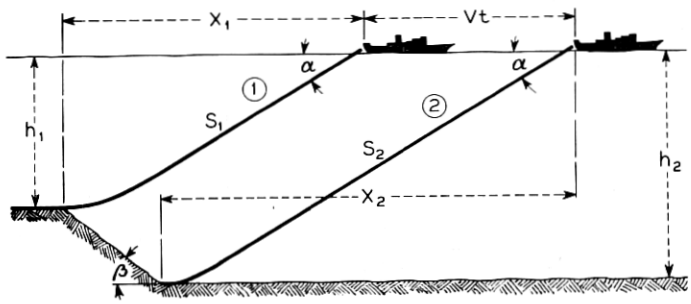

Fig. 24 — Piano wire configurations at the beginning and end of a descent lay.

Equations (39), (40), and (41), together with the general equations (Section 3.6)

$$\begin{aligned} S &= \frac{h}{\sin \alpha} + \kappa \frac{T_0}{w}, \\ X &= \frac{h}{\tan \alpha} + \lambda \frac{T_0}{w}, \end{aligned} \tag{24}$$

allow one readily to solve for the average error $\bar{\epsilon}$ in the piano wire indication of ship ground speed. The result is

$$\bar{\epsilon} = \frac{\sin \alpha + \sin \beta - \kappa \sin \alpha \sin \beta}{\sin (\alpha + \beta) - \lambda \sin \alpha \sin \beta} - 1. \tag{42}$$

For the small values of α and β which normally occur during the laying of the piano wire, the terms $\lambda \sin \alpha \sin \beta$ and $\kappa \sin \alpha \sin \beta$ are negligible. Hence, the average error $\bar{\epsilon}$ is thus very nearly

$$\bar{\epsilon} = \frac{\sin \alpha + \sin \beta}{\sin (\alpha + \beta)} - 1, \tag{43}$$

which, as (30) indicates, coincides with the amount of fill which would be required to lay downhill with the straight-line or zero touchdown tension configuration. Equation (43) is in turn closely approximated by (Section 5.1)

$$\bar{\epsilon} = \frac{\alpha\beta}{2} = \frac{H\beta}{2V}. \tag{44}$$

Similarly, for ascent laying of the wire on a bottom which rises less steeply than the inclination of the wire (19b), we get

$$\bar{\epsilon} = \frac{\sin \alpha - \sin \gamma + \kappa \sin \alpha \sin \gamma}{\sin (\alpha - \gamma) + \lambda \sin \alpha \sin \gamma} - 1, \tag{45}$$

which is very nearly

$$\bar{\epsilon} = \frac{-\alpha\gamma}{2} = -\frac{H\gamma}{2V}. \tag{46}$$

Thus, in both the above cases, the error in the piano wire technique can be closely obtained by assuming that the configuration of the wire is a straight line during ascent and descent laying. This is not surprising since, as we saw in Section 3.6, the deviation from the straight-line configuration during piano wire laying is normally small.

Because of its smooth exterior, the normal or transverse drag coefficient of the piano wire probably can be obtained from published curves for flow past a smooth right circular cylinder as shown in Appendix B. For typical 12 gauge (0.0290 inch diameter) piano wire, these curves yield a value of C_D of 1.45 and an H value of 25.0 degree-knots. However, these values of C_D and H must be considered tentative until confirmed experimentally.

Knowing the wire's H value, we can compute the error of the ground speed caused by descent and ascent laying of the piano wire by means of (44) and (46). The result of this computation for $H = 25.0$ degree-knots is shown in Fig. 25.

When the ascent angle of the bottom exceeds the incidence angle of the wire, suspensions result and the error cannot be computed without

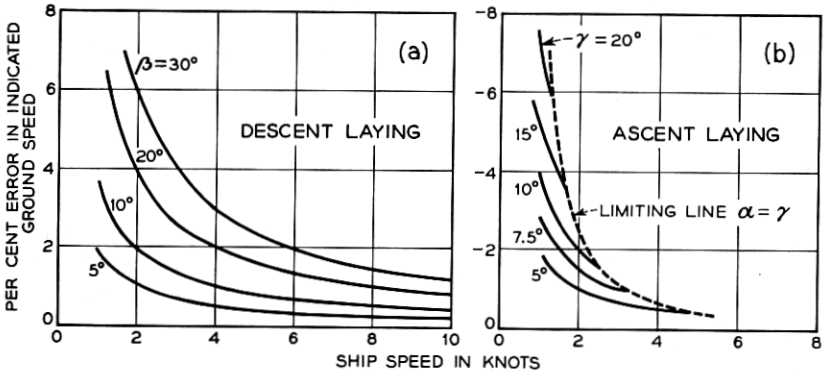

Fig. 25 — Error during descent and ascent laying of 12-gauge piano wire.

knowledge of the frictional properties of the bottom. For an H value of 25.0 degree-knots, (37) indicates that suspensions will occur for ship speeds V greater than $V = 25.0/\gamma$, where V is in knots and the ascent angle γ is in degrees. Hence, for a typical laying speed of 6 knots, ascent angles greater than 4.2 degrees will cause suspensions of the piano wire. These magnitudes indicate that suspensions of the piano wire probably actually develop in practice.

It is seen from Fig. 25 that for the usual small ascent or descent angles, the piano-wire technique is quite accurate, while for large bottom slopes it can be considerably in error. Again, however, if the bottom contour is known in advance, these errors can be estimated in the cases plotted in Fig. 25 and therefore can be corrected for. In this manner, the piano wire could be improved to give accurate ground speeds in all two-dimensional situations, with the exception of the case of a suspension caused by a too steeply ascending bottom. Such suspensions can be avoided only by maintaining a sufficiently slow ship speed. However, as seen by the small computed H value of 25.0 degree-knots, the ship speeds required to avoid piano wire suspensions on uneven bottoms are probably prohibitively slow. Hence, for steeply ascending bottoms it is likely that some other means of determining the ship ground speed is necessary.

VII. THREE-DIMENSIONAL STATIONARY MODEL

7.1 *General*

Thus far we have assumed that the cable lies entirely in the plane formed by the ship's velocity vector and the gravity vector. Because of the symmetry of the cable cross-section, this assumption seems reasonable.* However in certain cases, as for example in the presence of ocean cross-currents, the assumption of a planar configuration is clearly untenable. We consider therefore the case where the cable configuration is not necessarily planar but is still time independent with respect to a reference frame translating with the constant velocity of the ship. In analogy with previous terminology, we call this the three-dimensional stationary model.

Assume there is a constant velocity ocean current in each of a finite number of layers. Let the vector $\vec{V}_w$ denote the ocean-current velocity in a reference layer. In the stationary situation the velocity of the cable

* Because of asymmetries caused by the helical armor wire or because of minor out-of-roundness, it is conceivable that a sidewise drag force might develop which would cause the cable to move out of the ship's velocity-gravity plane. For a report of experimental observations of such yawing in wire stranded cables, see Reference 11.

configuration is everywhere the velocity of the ship, which we denote by the vector $\vec{V}$. Hence the velocity $\vec{V}'$ of the water with respect to the cable configuration in the reference layer is

$$\vec{V}' = \vec{V}_w + (-\vec{V}) = \vec{V}_w - \vec{V}.$$

Further, in this layer we choose a set of coordinate axes ξ, η, ζ translating at the velocity $\vec{V}$ as follows: The ξ axis has the direction of $-\vec{V}'$, while η is measured vertically upward, and ζ is perpendicular to η and ξ so that the axes ξ, η, ζ form a right-handed system. A plan view of this configuration is shown in Fig. 26. We have denoted the angle between $\vec{V}$ and $\vec{V}_w$ by β, while the angle between the ξ axis and $\vec{V}$ is denoted by φ. (The distances d and e refer to a subsequent section.) To describe the cable configuration with respect to the ξ, η, ζ axes, we use the spherical polar coordinates θ and ψ shown in Fig. 27. (The $\vec{t}, \vec{u}, \vec{v}$ vectors are discussed in Appendix F.)

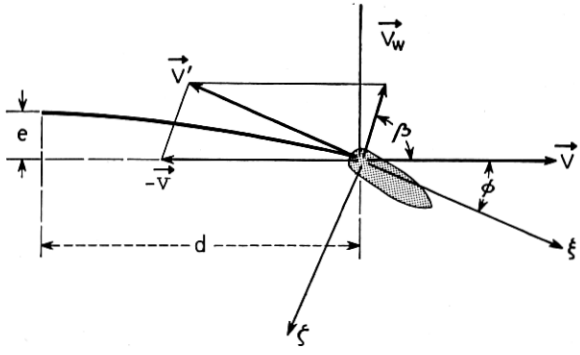

Fig. 26 — Plan view of the coordinate system for the three-dimensional stationary model.

As in the two-dimensional case, we resolve the velocity of the water with respect to a cable element in the reference layer into a component V_N normal to the cable and a component V_t tangential to the cable, and associate with V_N and V_t the drag forces D_N and D_T. The resulting differential equations, which are derived in detail in Appendix F, are the following:

$$(T - \rho_c V_c^2) \frac{d\theta}{ds}$$

$$+ w\Lambda'(\cos^2 \psi \sin^2 \theta + \sin^2 \psi)^{1/2} \cos \psi \sin \theta - w \cos \theta = 0, \quad \text{(a)}$$

$$(T - \rho_c V_c^2) \cos\theta \frac{d\psi}{ds} \tag{47}$$

$$+ w\Lambda'(\cos^2\psi \sin^2\theta + \sin^2\psi)^{1/2} \sin\psi = 0, \quad \text{(b)}$$

$$\frac{dT}{ds} + D_T - w \sin\theta = 0, \quad \text{(c)}$$

where $\Lambda' = C_D \rho d V'^2/2$, and V' is the magnitude of $\vec{V}'$.

In addition, connecting the coordinates $\xi(s)$, $\eta(s)$, and $\zeta(s)$ of a point s along the cable with the angles θ and ψ we have the geometric relationships

$$\frac{d\xi(s)}{ds} = \cos\theta \cos\psi, \quad \text{(a)}$$

$$\frac{d\eta(s)}{ds} = \sin\theta, \quad \text{(b)} \tag{48}$$

$$\frac{d\zeta(s)}{ds} = -\cos\theta \sin\psi. \quad \text{(c)}$$

Two important general results follow from (47) and (48). For one, if the tangential drag force D_T is negligibly small, (48b) substituted into equation (47c) yields upon integration

$$T = T_0 + w\eta, \tag{49}$$

where T_0 is the tension at $\eta = 0$. Hence, if η is measured from the ocean

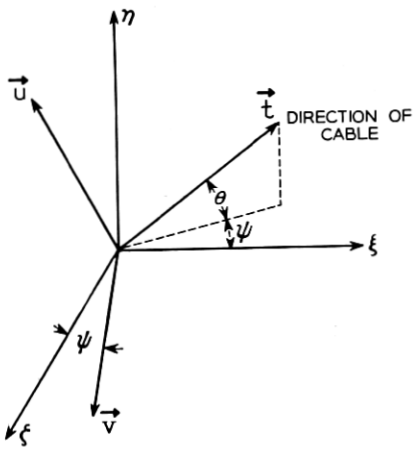

Fig. 27 — Definition of the spherical polar coordinates θ and ψ and the unit vectors $\vec{t}$, $\vec{u}$, and $\vec{v}$.

surface, and if at the bottom ($\eta = -h$) the tension is zero, the tension at the ship is essentially *wh*, *regardless* of the nature of the normal drag forces. Since in most laying situations for present cables, the tangential drag force can be reasonably neglected, this fact provides a convenient over-all check on the laying process. That is, if the cable is being laid with excess, the tension at the ship for *any* stationary cable configuration, *planar* or *non-planar*, should be essentially *wh*. Any marked increase of tension over the *wh* value necessarily means the bottom tension is non-zero and insufficient cable is being paid out.

The second important result is derived in Appendix F. This result is that if the bottom ocean layer in our model is devoid of cross currents, and if the bottom tension is zero, then, for the boundary conditions which are normally observed, the cable configuration in the bottom layer is a straight line. Further, this straight line is in the plane formed by the ship's velocity vector $\vec{V}$ and the gravity vector. Hence, for example, in laying with excess in a sea which contains surface currents, the cable configuration in the lower, current-free portion will be a straight line in a vertical plane parallel to the resultant velocity of the ship. The laid cable will be parallel to the ship's path, but displaced a certain distance from it. Thus, because the lower portion is a straight line, our previous results about the kinematics of straight-line laying still apply. Only they now are pertinent to the displaced bottom contour rather than to the contour which lies directly beneath the ship.

7.2 *Perturbation Solution for a Uniform Cross-Current*

Cross-currents are commonly confined to a region near the ocean surface. It is of interest therefore to determine for such surface currents the distance e (Fig. 26) which the laid cable will be displaced from the path of the ship. In Appendix F we consider the problem for a cross-current of uniform but comparatively small velocity. In addition, we determine the distance d (Fig. 26) back of the ship at which the cable leaves the upper, cross-current stratum and assumes the straight-line configuration it has in the lower stratum. Let us assume for the sake of reference that the resultant ship velocity V is due east, and that the cross-current V_w is inclined at an angle β to the north (Fig. 26). The resultant velocity V' of the water with respect to the cable in the surface stratum has the magnitude therefore of

$$V' = [(V - V_w \cos \beta)^2 + (V_w \sin \beta)^2]^{\frac{1}{2}}, \tag{50}$$

and is inclined at the angle φ from due west, where

$$\tan \varphi = \frac{V_w \sin \beta}{V - V_w \cos \beta}. \tag{51}$$

Associated with V' we have a critical angle α' which is given approximately by H/V' or exactly by (10) or (11).

In terms of φ, α', and α the analysis of Appendix F yields the following values of d and e.

$$\begin{aligned} d &= h'\left(\operatorname{ctn}\alpha' - \frac{\Delta\alpha}{2\cos^2\alpha'}\frac{h-h'}{h'}\left[1-\left(1-\frac{h'}{h}\right)^{2\operatorname{ctn}^2\alpha'}\right]\right) \quad \text{(a)} \\ e &= h'\varphi\operatorname{ctn}\alpha'\left(1-\frac{h-h'}{h'}\tan^2\alpha'\left[1-\left(1-\frac{h'}{h}\right)^{\operatorname{ctn}^2\alpha'}\right]\right), \quad \text{(b)} \end{aligned} \tag{52}$$

where $\Delta\alpha = \alpha - \alpha'$ is the difference of lower and upper stratum critical angles, h' is the depth of the upper, cross-current stratum and h is the total depth.* Curves from which d and e may be evaluated are given in Figs. 28 and 29 in dimensionless form. To illustrate their application we consider the following.

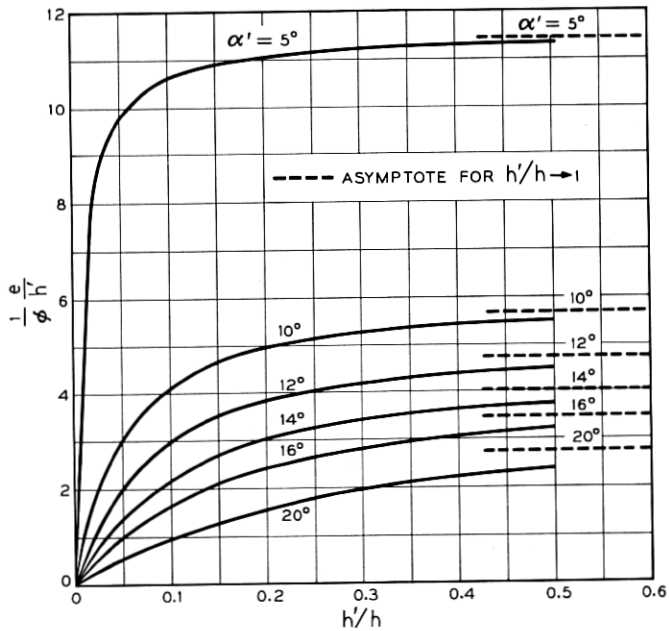

Fig. 28 — Distance the laid cable is offset from the ship's path.

* In Appendix F the equation of the space curve formed by the cable in the upper stratum is also given.

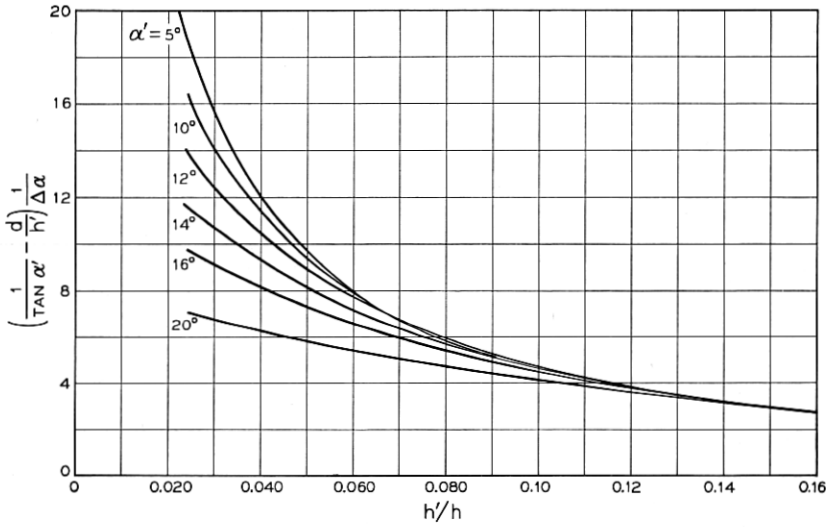

Fig. 29 — Distance behind the ship at which the cable enters the lower stratum.

Example: A ship is laying cable No. 2 at a depth of 6,000 ft at a resultant ground speed of 6 knots due east. There is a one knot cross-current 600 feet deep running 30° east of north. Find e and d.

Here $\beta = 60°$ and we obtain from (50) by a simple computation $V' = 5.57$ knots. Also since for cable No. 2 $H = 70$ degree-knots,

$$h'/h = 600/6000 = 0.1,$$

$$\alpha' = 70/5.57 = 12.3 \text{ degrees.}$$

By interpolation, we find from Figs. 28 and 29

$$\frac{1}{\varphi}\frac{e}{h'} = 2.7,$$

$$\left(\frac{1}{\tan \alpha'} - \frac{d}{h'}\right)\frac{1}{\Delta\alpha} = 4.7.$$

Equation (51) yields in turn $\varphi = 0.156$ radians, and $\Delta\alpha$ is given by

$$\Delta\alpha = \frac{70}{V} - \frac{70}{V'} = -0.6 \text{ degrees} = -0.010 \text{ radians.}$$

Hence, we have

$$e = 3.6\, h'\varphi = 2.7 \times 600 \times 0.156 = 253 \text{ ft},$$

$$d = h'\left[\frac{1}{\tan \alpha'} - 4.7\Delta\alpha\right] = 6000\,[4.59 + 4.7 \times 0.010] = 2800 \text{ ft.}$$

APPENDIX A

Discussion of the Two-Dimensional Stationary Configuration for Zero Bottom Tension

We assume again that the tangential drag D_T depends only on the relative tangential velocity V_T, and we consider in a T, θ plane the solution trajectories of equations (18). These trajectories satisfy the equation

$$\frac{dT}{d\theta} = \frac{(\sin\theta - D_T/w)}{\cos\theta - \Lambda \sin\theta \mid \sin\theta \mid} (T - \rho_c V_c^2), \tag{53}$$

and are periodic in θ with a period of 2π. In Fig. 30 we have plotted the solution trajectories qualitatively for $(\alpha - \pi) \leqq \theta \leqq (\alpha + \pi)$. It is seen that the trajectories are either the vertical straight lines $\theta = \alpha$, $\theta = \alpha \pm \pi$ or they lie completely within one of four regions, labelled I, II, III, or IV, which are bounded by these vertical lines and the horizontal line $T = \rho_c V_c^2$. The trajectory $\theta = \alpha$ corresponds to the straight-line laying configuration, while the trajectories $\theta = \alpha \pm \pi$ correspond to Shea's straight-line recovery method.

Examine now the trajectories in Regions II and III at a point of which $T = 0$. As J. F. Shea has pointed out, these trajectories all lie below the line $T = \rho_c V_c^2$. On the other hand, the trajectory $\theta = \alpha$ con-

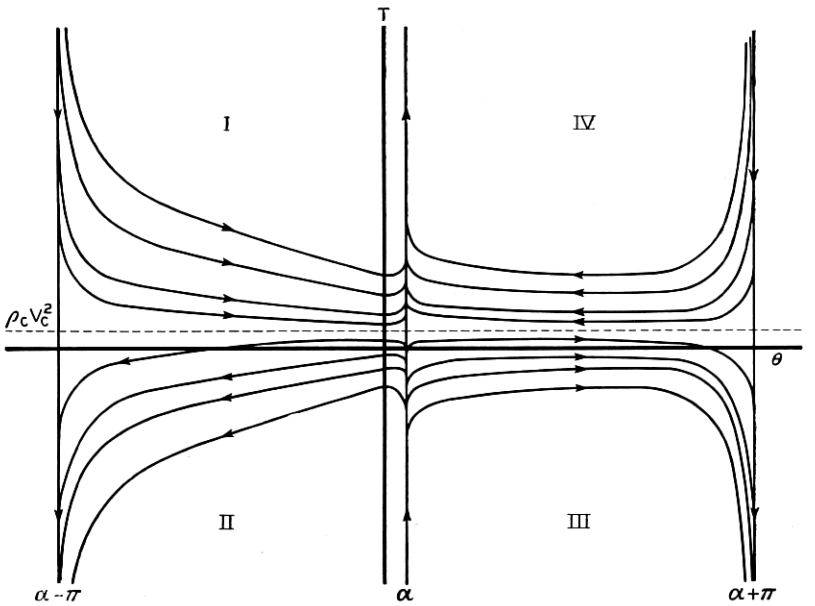

Fig. 30 — Qualitative representation of the solution trajectories of the two-dimensional stationary model.

tains all values of T. Hence, according to the stationary model, the only cable configuration for laying which has the value $T = 0$ and values of $T \geqq \rho_c V_c^2$ is the straight line inclined at the critical angle α. The magnitude of $\rho_c V_c^2$ is small. For example, for cable No. 2 paid out at six knots $\rho_c V_c^2$ is roughly six pounds, and for conditions approximating stationary laying the observed tensions at the ship are in practice always many times the $\rho_c V_c^2$ value. For such magnitudes of shipboard tensions and a zero bottom tension, the two-dimensional stationary model thus yields the straight line as the only possible cable configuration.

However, the empirical fact that $T > \rho_c V_c^2$ does not guarantee that the shipboard tension must be greater than $\rho_c V_c^2$. We might somehow contrive to lay at a zero bottom tension with $T < \rho_c V_c^2$ and with the cable in one of the non-straight line configurations of Regions II or III.

Consider the cable configuration lying in Region II. From Fig. 7 it can be seen that the vertical velocity of a cable element is given by

$$\frac{dy}{dt} = -V_{\text{vert}} = -V_c \sin \theta,$$

where y is measured upward. Hence, of the possible trajectories for which the bottom tension is zero only those for which the bottom cable angle θ_0 is between zero and π correspond to cable laying. For region II, therefore we need consider only the trajectories in the range $0 \leqq \theta_0 < \alpha$ at $T_0 = 0$. From (20c) the maximum value of y_m for these trajectories is given by

$$y_m = \frac{\rho_c V_c^2}{w} \int_0^{\theta_0} \left\{ \frac{\sin \xi}{(\cos \xi - \Lambda \sin^2 \xi)} \times \exp\left[- \int_\xi^{\theta_0} \frac{w \sin \eta - D_T(\eta)}{w (\cos \eta - \Lambda \sin^2 \eta)} \, d\eta \right] \right\} d\xi. \tag{54}$$

Let $(D_T)_m$ be the maximum value of D_T, $0 \leqq \eta < \alpha$. With D_T set equal to $(D_T)_m$, the right-hand side of (54) gives an upper bound on y_m. This substitution further allows one to evaluate the right-hand side of this equation in terms of standard integrals. The result yields the following upper bound on y_m:

$$y_m < 2.1 \frac{\rho_c V_c^2}{w} \frac{1}{1 - r},$$

where

$$r = \frac{(D_T)_m}{w \sin \alpha}.$$

In general, this upper bound will be much less than the laying depth. For example, for cable No. 2 being laid with 6 per cent slack at 6 knots $y_m < 12.5$ feet. That is, the cable configurations corresponding to Region II do not reach the ocean surface. Hence these solutions of the stationary model do not in general satisfy all the required boundary conditions and can be discarded.

Similarly, in Region III, the laying trajectories for which $T_0 = 0$ are in the range $\alpha < \theta_0 \leqq \pi$. Consider those for which $\theta_0 < \pi/2$. We get for these trajectories

$$y_{\pi/2} = \frac{\rho_c V_c^2}{w} \int_{\theta_0}^{\pi/2} \left\{ \frac{\sin \xi}{(\Lambda \sin^2 \xi - \cos \xi)} \times \exp\left[- \int_{\theta_0}^{\xi} \frac{w \sin \eta - D_T(\eta)}{w (\Lambda \sin^2 \eta - \cos \eta)} \, d\eta \right] \right\} d\xi, \tag{55}$$

where $y_{\pi/2}$ is the value of y at $\theta = \pi/2$. Let m be the minimum value of $\sin \eta - (D_T(\eta)/w)$ in the range $\alpha < \eta \leqq \pi/2$. If, as in the usual case, m is positive, we can obtain an upper bound on $y_{\pi/2}$ by replacing $\sin \eta - (D_T(\eta)/w)$ by m in the right-hand side of (55). By this means we find that

$$y_{\pi/2} < \frac{\rho_c V_c^2}{w} \frac{2(1 + \cos^2 \alpha)}{m \tan \alpha/2}.$$

For cable No. 2 being laid with 6 per cent slack at 6 knots this relation yields $y_{\pi/2} < 1{,}100$ feet. So in the usual laying depths, which are many times greater than $y_{\pi/2}$, the configurations in Region III for which $T_0 = 0$ correspond to a value of θ at the surface greater than $\pi/2$, or to cable being paid out *in front* of the ship during laying. It is doubtful whether such configurations would be stable and, at any rate, doubtful whether cable would ever be laid in such a manner. Hence, we conclude that these $T_0 = 0$ solutions of Regions II and III will in general be mathematical curiosities, and that the only realistic laying solution of the stationary model for which the bottom tension is zero is the straight line $\theta \equiv \alpha$.

APPENDIX B

Computation of the Transverse Drag Coefficient and the Hydrodynamic Constant of a Smooth Cable from Published Data

From (6) of Section 3.2 we obtain the relationship

$$\frac{V \sin \alpha}{\sqrt{\cos \alpha}} = \left(\frac{2w}{C_D \rho d}\right)^{1/2} = H, \tag{56}$$

where H is the hydrodynamic constant. Also, we define the Reynolds number for flow normal to the cable in the usual way;

$$N_R = \frac{dV \sin \alpha}{\nu}, \tag{57}$$

ν being the kinematic viscosity of water. For smooth cable we now assume that the drag coefficient C_D depends on N_R in the same way as for flow around a smooth cylinder of infinite length. Experimental data for this relationship, namely,

$$C_D = C_D(N_R) \tag{58}$$

are available in the literature and have been collated by Eisner.[15]

For a given velocity V, (56) through (58) represent three equations for the unknowns α, C_D, and N_R. In general, the solution of these equations depends on V, thus contradicting the assumption made in Section 3.2 that C_D, and therefore H, are constants independent of V. However, for sufficiently large V we can expect the resulting α to be small so that $\sqrt{\cos \alpha} \approx 1$. In this case (56) and (57) combine to give

$$C_D = \frac{2wd}{\rho \nu^2} \frac{1}{N_R^2}, \tag{59}$$

which together with (58) yields two equations for C_D and N_R that are indeed independent of V. In laying, V will normally be large enough for this approximation to hold.

Equations (58) and (59) are in turn easily solved graphically by finding the intersection on log-log paper of the curves, C_D versus N_R, that these equations represent. Since ρ and ν are properties only of the water, we see that C_D is a function only of the product wd of the unit weight of the cable times its diameter. In Fig. 31 we have plotted the resulting values of C_D for wd ranging from 10^{-7} to 10 pounds. For this computation we have assumed sea water at 32°F with an assumed density of 1.994 slugs per cubic foot and a kinematic viscosity of 2.006×10^{-5} ft^2/sec.

For other than large values of V, (56) through (58) can be readily solved if one interchanges the roles of α and V, that is, if one considers α as given and V as unknown. Equations (56) and (57) can again be combined in this case to give

$$C_D = \frac{2wd \cos \alpha}{\rho v^2} \frac{1}{N_R^2}, \tag{60}$$

and with $wd \cos \alpha$ a known number, (60) and (58) can be solved for C_D and N_R as before. Thus, one can obtain C_D from Figure 31 by merely reading $wd \cos \alpha$ rather than wd on the abscissa. Knowing C_D one can solve for V from (56).

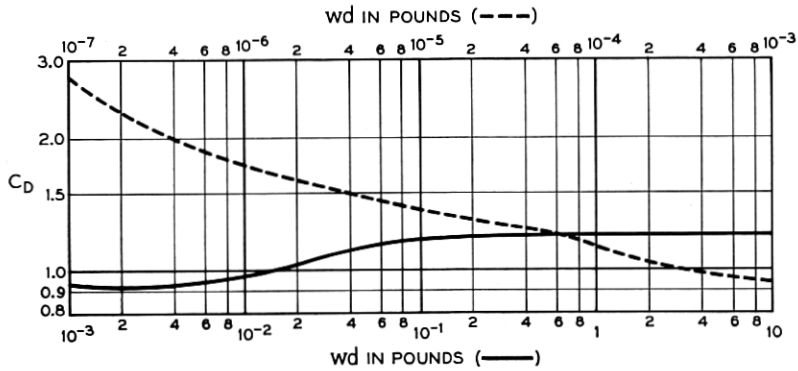

Fig. 31 — Variation of C_D with wd for cables of smooth exterior.

The results of such a computation are shown in Table II for cable No. 1. For $V > 1.5$ knots the experimentally determined H is 64.0 degree-knots. The corresponding computed values of H, ranging from 67.4 to 70.0 degree-knots, compare favorably with this experimental value. Over the entire range of V, from 0.25 to 10.00 knots, the variation in H is about 4 per cent. This small variation makes the assumption of Section 3.2 that H is a constant for all V appear reasonable, especially since we can only hope to use this computation in a preliminary design before the hydrodynamic properties of a cable are established by experiment.

TABLE II — COMPUTED VALUES OF N_R, C_D, AND H FOR CABLE NO. 1

V (knots)	N_R	C_D	H (deg.-knots)
0.25	1.25×10^3	0.935	67.5
0.50	2.50	0.922	70.0
1.50	5.20	0.965	67.8
3.00	5.80	0.985	67.5
10.00	6.05	1.000	67.4

In Table III we have indicated computed high-velocity H values as a function of the unit weight w and the diameter d of a cable. Table IV shows the computed high-velocity C_D and H for various gauge piano wire. The American Steel and Wire gauge scale is used in this tabulation.

TABLE III — COMPUTED VALUES OF THE HYDRODYNAMIC CONSTANT H IN DEGREE-KNOTS FOR SMOOTH CABLE

Submerged Weight in lb/ft	Diameter in Inches									
	0.5	0.75	1.00	1.25	1.50	1.75	2.0	2.5	3.0	4.0
0.1	54.5	44.2	37.9	33.7	30.6	28.1	26.2	23.2	21.0	17.9
0.2	75.9	61.1	52.3	46.4	41.9	38.5	35.8	31.6	28.5	24.4
0.3	91.7	73.6	62.9	55.6	50.2	46.1	42.8	38.0	34.4	29.7
0.4	104.7	83.9	71.5	63.1	57.1	52.5	48.9	43.5	39.6	34.3
0.5	115.9	92.6	78.9	69.8	63.3	58.3	54.4	48.5	44.3	38.3
0.6	125.8	100.4	85.6	75.9	68.9	63.6	59.5	53.2	48.5	42.0
0.7		107.6	91.9	81.6	74.2	68.7	64.2	57.4	52.4	45.3
0.8		114.2	97.8	87.0	79.3	73.4	68.6	61.3	55.9	48.4
0.9		120.6	103.4	92.1	84.1	77.8	72.7	65.0	59.3	51.3
1.0		126.5	108.7	97.1	88.6	82.0	76.6	68.5	62.5	54.1
2.0			153.3	137.0	125.0	115.7	108.2	96.7	88.2	76.3
3.0				167.6	152.9	141.5	132.3	118.2	107.9	93.3

TABLE IV — COMPUTED C_D AND H VALUES OF PIANO WIRE

Gauge (Am. Steel & Wire)	Dia. (inches)	C_D	H (deg- knots)
0	0.009	2.49	10.7
5	0.014	1.91	15.2
10	0.024	1.56	22.1
15	0.035	1.39	28.2
20	0.045	1.31	33.0
25	0.059	1.24	38.7
30	0.080	1.14	47.2
35	0.106	1.02	57.1
40	0.138	0.970	67.1

APPENDIX C

Some Approximate Solutions for Laying and Recovery

C.1 *Laying*

We assume that the tangential drag and the centrifugal forces are negligible. Then, since for laying $0 \leqq \theta \leqq \pi$, (18a) by virtue of (21) becomes

$$\left(\frac{T_0}{w} + y\right)\frac{d\theta}{ds} + \Lambda \sin^2\theta - \cos\theta = 0. \tag{61}$$

Let the origin of an x, y coordinate system be at the cable touchdown point (Fig. 8). Further, let x be the x coordinate of a point along the cable configuration and s the corresponding distance along the cable from the origin. If we define

$$\Delta = s - x, \tag{62}$$

then

$$\frac{d\Delta}{dy} = \frac{ds}{dy} - \frac{dx}{dy} = \tan\frac{\theta}{2}, \tag{63}$$

and

$$\frac{dy}{ds} = \sin\theta. \tag{64}$$

By means of (63) and (64), (61) transforms to

$$(\overline{T}_0 + \bar{y})\frac{d\bar{\Delta}}{d\bar{y}}\frac{d^2\bar{\Delta}}{d\bar{y}^2} + \frac{1}{4}\frac{(d\bar{\Delta})^4}{(d\bar{y})} + \Lambda\frac{(d\bar{\Delta})^2}{(d\bar{y})} - \frac{1}{4} = 0, \tag{65}$$

where we have in addition introduced the non-dimensional variables

$$\overline{T}_0 = T_0/wh,$$

$$\bar{\Delta} = \Delta/h,$$

$$\bar{y} = y/h.$$

Here h is the ocean depth at the touchdown point. Using the condition that $\theta = 0$ at $y = 0$, which implies $d\Delta/dy = 0$ at $y = 0$, we get upon integrating (65)

$$\frac{d\bar{\Delta}}{d\bar{y}} = \tan\frac{\alpha}{2}\left(\frac{1 - [\overline{T}_0/(\overline{T}_0 + \bar{y})]^\gamma}{1 + [\overline{T}_0/(\overline{T}_0 + \bar{y})]^\gamma \tan^4\frac{\alpha}{2}}\right)^{1/2}, \tag{66}$$

where

$$\gamma = \frac{2 - \sin^2\alpha}{\sin^2\alpha}. \tag{67}$$

The usual range of the critical angle α is between 10 and 30 degrees. Also

$$0 \leqq \frac{\overline{T}_0}{\overline{T}_0 + \bar{y}} \leqq 1.$$

Therefore, we approximate the denominator of equation (67) by unity.

With the boundary condition that $\Delta = s - x = 0$ at $y = 0$, we thus obtain

$$\bar{\Delta}(1) = \bar{S} - \bar{X} = \tan\frac{\alpha}{2}\int_0^1 (1 - [\bar{T}_0/(\bar{T}_0 + \xi)]^\gamma)^{\frac{1}{2}}\, d\xi, \tag{68}$$

where $\bar{S}$ and $\bar{X}$ are the dimensionless values of s and x at the ship.

Next we let

$$\omega = s + x, \qquad \bar{\omega} = \omega/h.$$

Then we have

$$\frac{d\bar{\omega}}{d\bar{y}} = 1\Big/\frac{d\bar{\Delta}}{d\bar{y}},$$

and, as can be seen from (66) through (68),

$$\bar{\omega}(1) = \bar{S} + \bar{X} = \operatorname{ctn}\frac{\alpha}{2}\int_0^1 (1 - [\bar{T}_0/(T_0 + \xi)]^\gamma)^{-\frac{1}{2}}\, d\xi. \tag{69}$$

For convenience we define u and R by

$$u = \frac{\bar{T}_0}{\bar{T}_0 + \xi},$$

$$R = \frac{\bar{T}_0}{1 + \bar{T}_0}.$$

In terms of u and R (68) and (69) become

$$\bar{\Delta}(1) = \bar{T}_0 \tan\frac{\alpha}{2}\int_R^1 \frac{(1 - u^\gamma)^{\frac{1}{2}}}{u^2}\, du, \tag{70}$$

$$\bar{\omega}(1) = \bar{T}_0 \operatorname{ctn}\frac{\alpha}{2}\int_R^1 \frac{du}{u^2(1 - u^\gamma)^{\frac{1}{2}}}. \tag{71}$$

Further, integration by parts gives

$$\int_R^1 \frac{(1 - u^\gamma)^{\frac{1}{2}}}{u^2}\, du = \frac{(1 - R^\gamma)^{\frac{1}{2}}}{R} + \frac{\gamma}{2}\int_R^1 \frac{(1 - u^\gamma)^{\frac{1}{2}}}{u^2}\, du - \frac{\gamma}{2}\int_R^1 \frac{du}{u^2(1 - u^\gamma)^{\frac{1}{2}}}.$$

Combining the above three equations and making the approximation $(1 - R^\gamma)^{\frac{1}{2}} \approx 1$, we find

$$\left(1 - \frac{\gamma}{2}\right)\bar{\Delta}(1) + \frac{\gamma}{2}\tan^2\frac{\alpha}{2}\,\bar{\omega}(1) = (1 + \bar{T}_0)\tan\frac{\alpha}{2}. \tag{72}$$

Thus $\bar{\Delta}(1)$ and $\bar{\omega}(1)$ are related, and we need evaluate only one of the quantities numerically by means of equation (70) or (71) in order to compute both $\bar{\Delta}(1)$ and $\bar{\omega}(1)$, and hence $\bar{S}$ and $\bar{X}$.

The singularity at $u = 1$ makes the numerical evaluation of the integral in (71) cumbersome. Therefore we consider the evaluation of $\bar{\Delta}(1)$. But for convenience of numerical calculation we write (70) as

$$\bar{\Delta}(1) = -\bar{T}_0 \tan\frac{\alpha}{2}\int_R^1 (1-u^\gamma)^{\frac{1}{2}}\, d\left(\frac{1-u}{u}\right),$$

and integrate by parts to get

$$\bar{\Delta}(1) = \tan\frac{\alpha}{2}\left((1-R^\gamma)^{\frac{1}{2}} - \frac{\gamma}{2}\bar{T}_0\int_R^1 \frac{1-u}{u^2}\frac{u^\gamma}{(1-u^\gamma)^{\frac{1}{2}}}\, du\right).$$

We note again that $(1-R^\gamma)^{\frac{1}{2}} \approx 1$. Further, essentially all of contribution to the integral in this equation occurs near $u = 1$ because of the large value of γ. On the other hand, the values of $\bar{T}_0$ which are of interest will normally be smaller than unity. Hence R, the lower limit, will normally be less than one-half, and thus will be outside of the region of significant contribution to the integral. Therefore, we can take the integral to be a constant for a given α. Denoting this integral by n and combining these considerations we obtain

$$\bar{\Delta}(1) = \tan\frac{\alpha}{2} - \frac{\gamma}{2} n \tan\frac{\alpha}{2}\bar{T}_0. \tag{73}$$

Finally solving for $\bar{S}$ and $\bar{X}$ from (68) and (69), we find

$$\bar{S} = \frac{1}{\sin\alpha} + \kappa\bar{T}_0,$$

$$\bar{X} = \frac{1}{\tan\alpha} + \lambda\bar{T}_0,$$

which are a dimensionless form of (24). For brevity we have written

$$\kappa = \frac{1}{2}\left(\frac{2}{\lambda}\left[1 - \frac{\gamma}{2}\left(\frac{\gamma}{2}-1\right)n\right]\operatorname{ctn}\frac{\alpha}{2} - \frac{\gamma}{2} n \tan\frac{\alpha}{2}\right),$$

$$\lambda = \frac{1}{2}\left(\frac{2}{\gamma}\left[1 - \frac{\gamma}{2}\left(\frac{\gamma}{2}-1\right)n\right]\operatorname{ctn}\frac{\alpha}{2} + \frac{\gamma}{2} n \tan\frac{\alpha}{2}\right).$$

Since the integral n and the constant γ depend only on α, the constants κ and λ are also functions of α only. We have evaluated n by numerical integration and have plotted the resulting values of κ and $\lambda - \kappa$ in Fig. 10.

C.2 *Recovery*

In the conventional recovery situation we have as boundary conditions

$$\begin{aligned} \theta &= 0 \qquad \text{at} \quad y = 0, \\ \theta &= -\alpha_s \quad \text{at} \quad y = h, \end{aligned} \tag{74}$$

where α_s is the incidence angle of the cable at the ship (Fig. 8). With these boundary conditions, the development leading to (66) yields (26) for the relationship between shipboard tension $\overline{T}_s$ and the incidence angle α_s.

To evaluate S and X, the values of s and x at the ship, we use (19), (20a) and (20b). Again we simplify by assuming $D_T = \rho_c V_c^2 = 0$. Further, since for recovery $-\pi \leqq \theta \leqq 0$, we may write $|\sin \xi| = -\sin \xi$. This gives

$$\begin{aligned} \bar{S} &= \overline{T}_0 \int_0^{-\alpha_s} \left[\frac{1}{\cos \xi + \Lambda \sin^2 \xi} \exp \int_0^{\xi} \frac{\sin \eta}{\cos \eta + \Lambda \sin^2 \eta} \, d\eta \right] d\xi, \\ \bar{X} &= \overline{T}_0 \int_0^{-\alpha_s} \left[\frac{\cos \xi}{\cos \xi + \Lambda \sin^2 \xi} \exp \int_0^{\xi} \frac{\sin \eta}{\cos \eta + \Lambda \sin^2 \eta} \, d\eta \right] d\xi. \end{aligned} \tag{75}$$

The dimensionless bottom tension $\overline{T}_0$ is computed from (26). The integrals appearing in (75) have been evaluated numerically. The results are shown in Figs. 14 and 15.

APPENDIX D

Analysis of the Effect of Ship Motion

D.1 *Formulation of the Differential Equations*

To analyze the effect of ship motion on cable tensions, we use the model shown in Fig. 32. We assume the cable is a perfectly flexible and elastic string whose motion is planar. The distance L along the cable from the ship to the point of entry into the water is taken as constant, and the longitudinal damping as negligible.

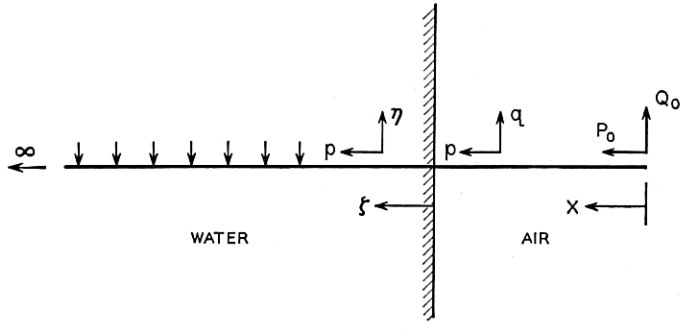

Fig. 32 — Model used for the analysis of ship motion tensions.

Unlike the solution of the basic stationary model, the complete solution of this model is not simple. To make the problem tractable, we shall make further simplifying assumptions. Although these assumptions may seem reasonable, they must be ultimately justified by comparison of experience with predicted results.

Force diagrams of a differential element of cable are shown in Figs. 33(a) and (b) for the two regions, air and water respectively. The notation is

p = longitudinal displacement of a point of the cable,
q = transverse displacement of a point of the cable (in air),
η = transverse displacement of a point of the cable (in water),
θ = the stationary angle, i.e. the angle the cable configuration makes with the ship velocity in the absence of ship motion,
φ = deviation from the stationary angle – positive in the clockwise direction,
s = distance along the stretched cable,
x = distance along the unstretched cable (in air),
ζ = distance along the unstretched cable (in water),
w_a = weight per unit length of cable in air.

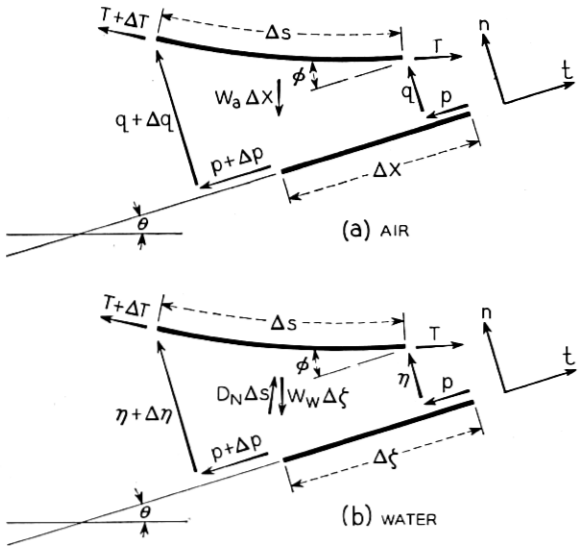

Fig. 33 — Diagram of forces acting on a cable element in air and in water.

Summing forces along the directions t (tangential) and n (normal) shown in Fig. 33, dividing by Δx (air) or $\Delta\zeta$ (water) and letting $\Delta x \to 0$ and $\Delta\zeta \to 0$, we obtain the following equations of equilibrium*

Air:

$$\begin{aligned} T\varphi_x - w_a \cos(\theta - \varphi) &= \rho_c(q_{tt}\cos\varphi - p_{tt}\sin\varphi), \\ T_x + w_a \sin(\theta - \varphi) &= \rho_c(q_{tt}\sin\varphi + p_{tt}\cos\varphi), \end{aligned} \tag{76}$$

Water:

$$\begin{aligned} T\varphi_\zeta + D_N s_\zeta - w\cos(\theta - \varphi) &= \rho_w(q_{tt}\cos\varphi - p_{tt}\sin\varphi), \\ T_\zeta + w\sin(\theta - \varphi) &= \rho_c(q_{tt}\sin\varphi + q_{tt}\cos\varphi). \end{aligned} \tag{77}$$

Here, ρ_c denotes the mass per unit length of the cable in air. As is known from hydrodynamic theory, in order to accelerate a body through a fluid, one must change not only the momentum of the body but that of some of the surrounding fluid as well. Thus the body has a virtual or apparent mass in addition to its intrinsic mass. In the first (77), the equation of equilibrium in the normal direction in water, we accordingly use ρ_w, given by

$$\rho_w = \rho_c + \frac{\pi}{4} d^2\rho$$

as the intrinsic plus virtual mass per unit length of cable moving through water. The quantities d and ρ are the outer diameter of the cable and mass density of the water, respectively, and the quantity $(\pi/4)d^2\rho$ is the virtual mass of a unit length circular cylinder moving transversely through water.

We take for the normal drag force per unit length

$$D_N = \frac{C_D\rho d}{2} V_N \mid V_N \mid. \tag{78}$$

Here V_N is the normal component of velocity of the water relative to the cable, i.e.,

$$V_N = V\sin(\theta - \varphi) + u_t \sin\varphi - \eta_t\cos\varphi, \tag{79}$$

and $C_D\rho d/2$ is a constant.

The quantities s and φ are given by the following geometric relations which can be obtained from Fig. 33:

* We use the subscript notation for differentiation throughout this section, e.g., $\varphi_x = \partial\varphi/\partial x$.

$$s_\zeta = [(1 + p_\zeta)^2 + \eta_\zeta^2]^{\frac{1}{2}} \tag{80}$$

$$\tan \varphi = \eta_\zeta/(1 + \eta_\zeta), \tag{81}$$

with similar expressions obtaining for the cable in air.

The tension T in turn is given by the Hooke's Law or stress-strain relation

$$\begin{aligned} T &= \overline{EA}\{[(1 + p_x)^2 + q_x^2]^{\frac{1}{2}} - 1\}, \qquad \text{(air)} \\ T &= \overline{EA}\{[(1 + p_\zeta)^2 + \eta_\zeta^2]^{\frac{1}{2}} - 1\}. \qquad \text{(water)} \end{aligned} \tag{82}$$

As we indicated in Section 4.1, we shall assume that the extensile rigidities $\overline{EA}$ corresponding to complete restraint and no restraint to twisting will give the limiting values of the ship motion tension.

Equations (76) through (82) form a complete system in terms of the independent variables x or ζ and t. Formulating boundary conditions in terms of the coordinate x (or ζ) is awkward. This coordinate is measured along the unstretched cable so that a disturbance applied at the ship is applied at different x's as the cable is paid out. At the same time, if the velocity of the pay-out is small compared to the significant wave velocity of the cable then we can plausibly neglect the paying out effect. As will be shown subsequently, in the problem at hand there are two significant wave velocities, roughly corresponding to transverse and longitudinal motion. The first of these is of the order of 200 ft/sec, while the second is of the order of 5,000–10,000 ft/sec. On the other hand, the pay-out velocity is of the order of 10 ft/sec. Hence, we take the pay-out velocity to be zero. This allows us to use (76) through (82) without further transformations and to identify x and ζ as coordinates fixed in the translating reference frame.

D.2 *Perturbation Equations*

We assume that the motion is a small perturbation about the undisturbed configuration of our model. To determine which terms of the differential equations are important in this case, we adopt the following procedure. Let

$$M = \max[(P_0 + P_1)^2 + Q_0^2]^{\frac{1}{2}},$$

where P_0 and Q_0 are displacements of the cable at the ship, and P_1 is the variation of the pay-out displacement from the mean. The quantity $e = M/L$ will normally be less than unity, and for no ship motion will be

zero. We write

$$P_0 + P_1 = af(t),$$
$$Q_0 = bg(t),$$

where $f(t)$, $g(t)$ are some bounded functions of time and a and b are constants. We assume that for given $f(t)$ and $g(t)$, T, p, and q vary analytically with e, namely

$$\begin{aligned} T &= T_0 + eT_1 + e^2T_2 + \cdots, \\ q &= eq_1 + e^2q_2 + \cdots, \\ p &= p_0 + ep_1 + e^2p_2 + \cdots, \end{aligned} \tag{83}$$

with counterparts for the submerged cable. The stationary transverse deflection is further assumed zero, and therefore the series for q contains no q_0 term. Substituting, for example, (83) into (82) for air and equating like powers of e, we find

$$\begin{aligned} T_0 &= \overline{EA}\,p_{0x}, && \text{(a)} \\ T_1 &= \overline{EA}\,p_{1x}, && \text{(b)} \\ T_2 &= \overline{EA}\left[p_{2x} + \frac{q_{1x}^2}{1 + p_{0x}}\right]. && \text{(c)} \end{aligned} \tag{84}$$

Equation (84a) of this sequence shows that only longitudinal displacements are associated with stationary tensions, while (84b) indicates that for small ship motions cable tensions are independent of the transverse component of ship motion. To compute the effect of transverse motion, (84c) shows that terms of the order e^2 in p and e in q must be considered. We assume further that $1 + p_{0x} \approx 1$, since p_{0x} is the order of magnitude of a strain.

Equations (83) and (84) substituted into (76) yield with this approximation

$$\begin{aligned} w_a \cos\alpha &= 0, && \text{(a)} \\ \overline{EA}\,p_{0xx} - \rho_a\,p_{0tt} + w_a \sin\alpha &= 0, && \text{(b)} \end{aligned} \tag{85}$$

$$\begin{aligned} q_{1xx} - \frac{1}{c_2^2}\,q_{1tt} &= 0, && \text{(a)} \\ p_{1xx} - \frac{1}{c_1^2}\,p_{1tt} &= 0, && \text{(b)} \\ p_{2xx} - \frac{1}{c_1^2}\,p_{2tt} &= \frac{1}{c_1^2}\,q_{1tt}q_{1xx} - q_{1x}q_{1xx}, && \text{(c)} \end{aligned} \tag{86}$$

where

$$c_1^2 = \overline{EA}/\rho_a ,$$

$$c_2^2 = T_0/\rho_a .$$

For non-zero w_a and $\alpha \neq \pi/2$, (85a) cannot be satisfied. This is a consequence of the assumption of $q_0 = 0$. With $p_{0tt} = 0$, equation (b) implies in turn that $T_0 =$ constant, which agrees with our model. For the submerged part of the cable, the equations do not yield a constant T_0 and thus contradict the assumed model. However, on the assumption that the transverse motion is confined to a region near the surface, we consider T_0 to be constant in the submerged part of the cable as well. We thus arrive at

$$\eta_{1\xi\xi} - \delta\eta_{1\xi} - \gamma\eta_{1t} - \frac{1}{\bar{c}_2^2}\eta_{1tt} = 0 \qquad \text{(a)}$$

$$p_{1\xi\xi} - \frac{1}{c_1^2}p_{1tt} = 0, \qquad \text{(b)} \quad (87)$$

$$p_{2\xi\xi} - \frac{1}{c_1^2}p_{2tt} = \frac{1}{c_1^2}\eta_{1tt}\eta_{1\xi} - \eta_{1\xi}\eta_{1\xi\xi} , \qquad \text{(c)}$$

where

$$\bar{c}_2^2 = T_0/\rho_w ,$$

$$\delta = \frac{C_D\rho\, dV^2}{T_0}\cos\alpha \sin\alpha,$$

$$\gamma = \frac{C_D\rho\, dV^2}{T_0}\sin\alpha,$$

as the differential equations governing the motion of the submerged cable. The constant c_1 is the velocity of propagation of a longitudinal wave in the cable, while the constants c_2 and $\bar{c}_2$ represent the propagation velocities of a transverse wave in air and water respectively.

D.3 *Solution of the Perturbation Equations*

We write

$$p(0, t) = P_0(t) + P_1(t),$$

$$q(0, t) = Q_0(t),$$

and take as boundary conditions

$$\begin{aligned} p_1(0, t) &= \frac{P_0(t) + P_1(t)}{e}, && \text{(a)} \\ p_2(0, t) &= 0, && \text{(b)} \\ q_1(0, t) &= Q_0/e. && \text{(c)} \end{aligned} \tag{88}$$

That is, we apportion all of the longitudinal boundary motion to p_1, and all of the transverse boundary motion to q_1. Equations [(84b), (86b) and (87b)] then give the complete tension due to the longitudinal component of ship motion to first order. As mentioned in the text, this tension is easily obtained from standard references, and is also the greater part of the ship motion tension.

To determine the tensions due to transverse ship motion, we solve (86c) and (87c) for boundary conditions (88b) and (88c). In addition, we have the transition conditions

$$\begin{aligned} q_1(L, t) &= \eta_1(0, t), && \text{(a)} \\ q_{1x}(L, t) &= \eta_{1\zeta}(0, t), && \text{(b)} \\ p_2(x = L, t) &= p_2(\zeta = 0, t), && \text{(c)} \\ p_{2x}(L, t) &= p_{2\zeta}(0, t), && \text{(d)} \end{aligned} \tag{89}$$

which follow if we assume that at the point of entry into the water the cable is continuous and the tensions are finite and continuous.

We consider only the problem of the tensions associated with a harmonic steady-state transverse disturbance. Equations (86a) and (87a) show the transverse response to this disturbance to be independent of the longitudinal motion to first order. The first-order transverse motion in turn can be thought of as a forcing action on the second order longitudinal motion, as (86c) and (87c) indicate. This suggests the program we follow to compute tensions. Namely, we first determine the first-order steady-state transverse response, then the second-order steady-state longitudinal response which is excited by the first-order transverse oscillation, and finally, by (84c) the resulting tension caused by transverse motion.

D.4 *Transverse Response*

At the ship we assume a harmonic forcing function

$$Q_0(t) = A \cos \omega t, \tag{90}$$

and we introduce complex exponential representation

$$q_1 = \text{Re } Q_1(x)\, e^{i\omega t},$$

$$\eta_1 = \text{Re } H_1(\zeta)\, e^{i\omega t},$$

where the factor $e^{i\omega t}$ will be henceforth suppressed.

The solution of (86a) and (87a) for the steady state may then be written

$$Q_1(x) = B_1 \exp \frac{i\omega x}{c_2} + B_2 \exp\left(-\frac{i\omega x}{c_2}\right),$$

$$H_1(\zeta) = F_1 \exp(q_1\zeta) + F_2 \exp(q_2\zeta),$$

where the B's and F's are complex constants and q_1 and q_2 are the roots of the quadratic

$$q^2 - \delta q - i\omega\gamma + \frac{\omega^2}{\bar{c}_2{}^2} = 0.$$

Throwing away the root of this equation which corresponds to the incoming wave in water, we get

$$H_1(\zeta) = F \exp(q_1\zeta).$$

where q_1 is the root corresponding to the outgoing wave. The three complex constants B_1, B_2, and F can now be determined from (89a), (89b) and (90)

$$\begin{aligned} B_1 + B_2 &= A/e, \\ B_1 \exp\frac{i\omega L}{c_2} + B_2 \exp\left(-\frac{i\omega L}{c_2}\right) - F &= 0, \\ \frac{i\omega}{c_2}\left[B_1 \exp\frac{i\omega L}{c_2} - B_2 \exp\left(-\frac{i\omega L}{c_2}\right)\right] - q_1 F &= 0. \end{aligned} \tag{91}$$

We note that B_1, B_2 and F are proportional to the amplitude A of the forcing motion.

D.5 *Second-Order Longitudinal Response*

From the preceding results, the right-hand sides of the equations of longitudinal motion (86c) and (87c) can be computed. This computation for (86c) results in

$$\frac{1}{c_1^2} v_{1tt} v_{1x} - v_{1xx} v_{1x} = \frac{1}{2}\left(\frac{c_2^2}{c_1^2} - 1\right)\left(\frac{\omega}{c_2}\right)^3 \times \left[\left(r_1 \sin \frac{2\omega x}{c_2} + r_2 \cos \frac{2\omega x}{c_2}\right) \cos 2\omega t + \left(r_3 \cos \frac{2\omega x}{c_2} - r_4 \sin \frac{2\omega x}{c_2}\right) \sin 2\omega t + r_5 \sin \frac{2\omega x}{c_2} + r_2 \cos \frac{2\omega x}{c_2}\right], \tag{92}$$

where the r's, which are proportional to the square of the amplitude A, are

$$r_1 = \text{Re}\,(B_1^2 + B_2^2),$$
$$r_2 = \text{Im}\,(B_1^2 - B_2^2),$$
$$r_3 = \text{Re}\,(B_1^2 - B_2^2),$$
$$r_4 = \text{Im}\,(B_1^2 + B_2^2),$$
$$r_5 = 2\text{Re}\, B_1 \bar{B}_2,$$
$$r_6 = r_5 + \frac{e^2 r_2^2}{A^2}.$$

[The quantity r_6 will be used subsequently.] Similarly, for the right-hand side of (87c) we get

$$\eta_{1\xi}\left(\frac{1}{c_1^2}\eta_{1tt} - \eta_{1\xi\xi}\right) = e^{-2\rho\xi}[(a_1 \cos 2\sigma\zeta + a_2 \sin 2\sigma\zeta) \cos 2\omega t + (a_1 \sin 2\sigma\zeta - a_2 \cos 2\sigma\zeta) \sin 2\omega t + a_3], \tag{93}$$

where

$$q_1 = -(\rho + i\sigma),$$
$$a_1 = \frac{|F|^2}{2} |q_1| \left[\left(\frac{\omega}{c_1}\right)^2 \cos(2f + g) + |q_1|^2 \cos(2f + 3g)\right],$$
$$a_2 = \frac{|F|^2}{2} |q_1| \left[\left(\frac{\omega}{c_1}\right)^2 \sin(2f + g) + |q_1|^2 \sin(2f + 3g)\right],$$
$$a_3 = |F| \left[\left(\frac{\omega}{c_1}\right)^2 + |q_1|^2\right] \rho,$$

and

$$f = \arg F, \qquad 0 \leqq f \leqq 2\pi,$$

$$g = \arg(-q_1), \qquad 0 \leqq g \leqq \frac{\pi}{2}.$$

It is seen that expression (92) and (93) have terms of the form

$$F(x)\begin{cases}\sin 2\omega t \\ \cos 2\omega t\end{cases} \tag{94}$$

in addition to functions of x (or ζ) alone. In accordance with the idea that the first order transverse motion is a forcing action on the second order longitudinal motion, we take as solutions of (86c) and (87c) functions of the form

$$G(x)\begin{cases}\sin 2\omega t \\ \cos 2\omega t\end{cases}$$

to correspond to terms of the type given by (94) and functions of x (or ζ) alone to correspond to forcing terms which are independent of time. This again gives linear differential equations which can be readily solved. For example, corresponding to the first term in (92) multiplying $\cos 2\omega t$ we have the assumed solution

$$G(x) \cos 2\omega t,$$

and the differential equation

$$\frac{d^2G}{dx^2} + \frac{4\omega^2}{c_1^2} G = \frac{1}{2}\left[\left(\frac{c_2}{c_1}\right)^2 - 1\right]\left(\frac{\omega}{c_2}\right)^3 \left[r_1 \sin\frac{2\omega x}{c_2} + r_2 \cos\frac{2\omega x}{c_2}\right].$$

This has the solution

$$G = \left[A_1 \cos\frac{\omega x}{c_1} + A_2 \sin\frac{\omega x}{c_1} + \frac{\omega}{8c_2}\left(r_1 \sin\frac{2\omega x}{c_2} + r_2 \cos\frac{2\omega x}{c_2}\right)\right],$$

where A_1 and A_2 are undetermined constants.

In this manner, the solution for the longitudinal motion can be obtained in terms of a set of constants. These in turn can be evaluated by means of the boundary and transition conditions on p_2. This evaluation, although straightforward, is very tedious. We shall omit the details of it here. The final result is

Air:

$$e^2T_2 = \frac{e^2\omega^2\overline{EA}}{4c_1c_2}\left\{\left[r_2\sin\frac{2\omega x}{c_1} + \left(r_3 + \frac{c_1}{c_2}r_4\sin\frac{2\omega L}{c_1} - \frac{c_1}{c_2}r_6\cos\frac{2\omega L}{c_1}\right)\cos\frac{2\omega x}{c_1} + \frac{c_1}{c_2}r_6\right]\cos 2\omega t + \left[r_3\sin\frac{2\omega L}{c_1} - \left(r_2 + \frac{c_1}{c_2}r_4\cos\frac{2\omega L}{c_1} + \frac{c_1}{c_2}r_6\sin\frac{2\omega L}{c_1}\right)\cos\frac{2\omega x}{c_1} + \frac{c_1}{c_2}r_4\right]\sin 2\omega t + \frac{c_2}{c_1}\left[r_5\left(\cos\frac{2\omega x}{c_2} - \cos\frac{2\omega L}{c_2}\right) - r_2\left(\sin\frac{2\omega x}{c_2} - \sin\frac{2\omega L}{c_2}\right) - \frac{|F|^2}{4}\right]\right\},$$

Water:

$$e^2T_2 = \frac{e^2\omega^2\overline{EA}}{4c_1c_2}\left\{\left[-r_2\cos\frac{2\omega L}{c_1} + r_3\sin\frac{2\omega L}{c_1} + \frac{c_1}{c_2}\sin\frac{2\omega L}{c_1}\left(r_4\sin\frac{2\omega L}{c_1} - r_6\cos\frac{2\omega L}{c_1}\right)\right]\sin 2\omega\left(t - \frac{\zeta}{c_1}\right) + \left[r_2\sin\frac{2\omega L}{c_1} + r_3\cos\frac{2\omega L}{c_1} + \frac{c_1}{c_2}\sin\frac{2\omega L}{c_1}\left(r_6\sin\frac{2\omega L}{c_1} + r_4\cos\frac{2\omega L}{c_1}\right)\right]\cos 2\omega\left(t - \frac{\zeta}{c_1}\right) - |F|^2\frac{c_2}{c_1}e^{-2\rho\zeta}\right\}.$$

D.6 *Numerical Results*

Since the r's are each proportional to the square of the amplitude A, the above results indicate that the transverse motion tension varies as A squared also. It is additionally a function of the frequency of ship motion ω, the forward mean ship velocity V, and the stationary tension T_0. The computation of the transverse ship motion tension for the laying situation was carried out for cable No. 2. The results are shown in Fig. 34. Here we have denoted the transverse motion tension by T_q and have plotted T_q/A^2 against the period of ship motion τ. Rather than the stationary tension T_0, we have used the depth h, which during laying is directly related to T_0 by $h = T_0/w$. Fig. 34(a) is a plot of T_q/A^2 versus the period $\tau = 2\pi/\omega$ for $h = \frac{1}{2}$, 2 and 3 nautical miles and for $V = 6$ knots. Figure 34(b) is a plot of T_q/A^2 versus τ for $V = 3$, 6, and 9 knots and $h =$ one nautical mile.

For representative laying, for example at 6 knots with a ship period of 6 seconds into a depth of one nautical mile, Fig. 34 gives

$$T_q/A^2 = 0.50 \text{ lb/ft}^2 \text{ (twist unrestrained)},$$

$$T_q/A^2 = 0.93 \text{ lb/ft}^2 \text{ (twist restrained)}.$$

For an extreme value of $A = 20$ feet, we get therefore that T_q is between 200 and 370 pounds.

Additionally, by means of the above analysis, one can compute the rate of damping of a transverse disturbance after it enters the water. The results of this computation are shown in Fig. 18 and are discussed in Section 4.1.

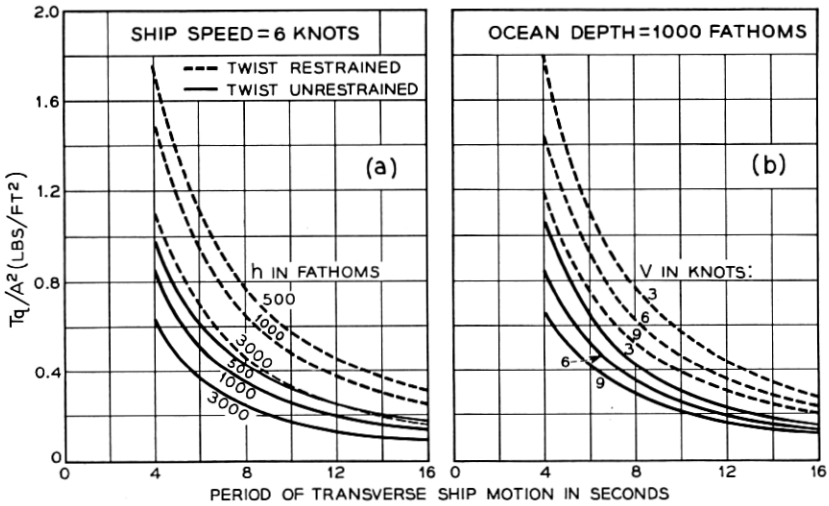

Fig. 34 — Variation of the transverse ship motion tension of cable No. 2 with the period of ship motion.

APPENDIX E

Tension Rise with Time for Suspended Cable

E.1 *Formulation of the Solution of the Problem*

Let O be the lowest point of the cable at time t after the suspension has begun (Fig. 35). We make the following definitions:

h = depth at onset of the suspension,

S_1 = cable length from A to 0,

S_2 = cable length from ship at B to 0,

X_1 = horizontal distance from A to 0,

X_2 = horizontal distance from B to 0,

δ = vertical distance from A to 0,

T_0 = cable tension at 0.

If the cable is being paid out with a slack ϵ, then conservation of the total cable length gives the equation

$$S_1 + S_2 = \frac{h}{\sin \alpha} + (1 + \epsilon)Vt + \text{cable stretching}. \tag{95}$$

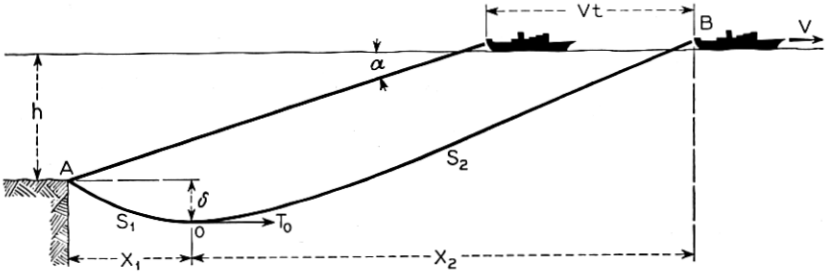

Fig. 35 — Coordinates for the analysis of tension rise when a cable is completely suspended.

It is assumed that there is no cable pulled from the bottom. The cable stretching we evaluate as in the example of Section 3.6, viz.,

$$\text{cable stretching} = (S_1 + S_2)\frac{T_0}{EA}.$$

This makes (95) read

$$S_1 + S_2 = \frac{h}{\sin \alpha} + (1 + \epsilon)Vt + (S_1 + S_2)\frac{T_0}{EA}. \tag{96}$$

To obtain further relations for the unknowns appearing in (96), we assume that from the ship to point 0 the cable configuration is a stationary one governed by the equations developed in Section 3.6, while from points 0 to A we assume that the cable configuration is a static catenary. These assumptions yield the following relations:

$$S_1 = \frac{T_0}{w}\sinh \sigma, \tag{a}$$

$$S_2 = \frac{h + \delta}{\sin \alpha} + \kappa\frac{T_0}{w}, \tag{b}$$

$$X_2 = \frac{h + \delta}{\tan \alpha} + \lambda \frac{T_0}{w}, \qquad \text{(c)}$$

$$\delta = \frac{T_0}{w} (\cosh \sigma - 1), \qquad \text{(d)} \qquad (97)$$

$$X_2 + X_1 = \frac{h}{\tan \alpha} + Vt, \qquad \text{(e)}$$

$$\sigma = \frac{wX_1}{T_0}, \qquad \text{(f)}$$

$$T_s = T_0 + w(h + \delta). \qquad \text{(g)}$$

Here κ and λ are constants, defined and plotted in Section 3.6, which depend only on α, the critical angle corresponding to V. Equations (96) and (97) form a complete set of equations in the unknowns X_1, X_2, S_1, S_2, T_0, T_s, δ, and σ. They can be reduced to a set which contain only the unknowns σ and T_s:

$$\varphi_1(\sigma) \sin \alpha - \epsilon\varphi_2(\sigma) \sin \alpha - \bar{h}\left(1 + \frac{\varphi_3(\sigma)}{\varphi_2(\sigma)} \bar{t} \sin \alpha\right) = 0, \qquad \text{(a)}$$

$$\overline{T}_s = 1 + \frac{\bar{t} \cosh \sigma}{\varphi_2(\sigma)}, \qquad \text{(b)} \qquad (98)$$

where

$$\bar{h} = wh/EA,$$

$$\bar{t} = Vt/h,$$

$$\overline{T}_s = T_s/wh,$$

and

$$\varphi_1 = \sinh \sigma - \sigma + (\cosh \sigma - 1) \tan \frac{\alpha}{2} - (\lambda - \kappa),$$

$$\varphi_2 = \frac{\cosh \sigma - 1}{\tan \alpha} + \lambda + \sigma,$$

$$\varphi_3 = \frac{\cosh \sigma - 1}{\sin \alpha} + \sinh \sigma.$$

A graphical iteration method will be used to solve (98). First we solve

$$\varphi_1(\sigma) \sin \alpha - \epsilon\varphi_2(\sigma) \sin \alpha - \bar{h} = 0 \qquad (99)$$

for σ by means of a nomograph to be described later. Next the quantities

$$\frac{\cosh \sigma}{\varphi_2(\sigma)}, \qquad \frac{\varphi_3(\sigma)}{\varphi_2(\sigma)} \sin \alpha,$$

are plotted as functions of σ for various α. These plots can then be used as follows to solve (98) for a given $\bar{t}$. Solve (99) to obtain σ_0. From the plot of $\varphi_3(\sigma)/\varphi_2(\sigma) \sin \alpha$ compute

$$\bar{h}_1^* = \bar{h}\left(1 + \frac{\varphi_3(\sigma_0)}{\varphi_2(\sigma_0)} \bar{t} \sin \alpha\right).$$

Using the value $\bar{h}_1^*$ for $\bar{h}$, compute σ_1 from (99). With this value of σ_1, compute h_2^* from

$$\bar{h}_2^* = \bar{h}\left(1 + \frac{\varphi_3(\sigma_1)}{\varphi_2(\sigma_1)} \bar{t} \sin \alpha\right),$$

etc. In this way a convergent sequence $\sigma_0, \sigma_1, \cdots, \sigma_n$ is generated. Finally, from the plot of $\cosh \sigma/\varphi_2(\sigma)$ obtain $\overline{T}_s$.

The above iteration procedure sounds tedious. Actually, in most cases the iteration is not necessary because σ remains essentially independent of time. Thus, the solution of (99) by means of the accompanying nomograph will usually give the complete solution of the problem.

E.2 *Nomograph (Alignment Chart) for the Solution of Equation* (99)

The relations

$$\begin{aligned} x_1 &= 0, \qquad x_2 = d, \qquad x_3 = \frac{10\varphi_2(\sigma)\, d \sin \alpha}{1 + 10\varphi_2(\sigma) \sin \alpha}, \\ y_1 &= \bar{h}, \qquad y_2 = \frac{\epsilon}{10}, \qquad y_3 = \frac{\varphi_1(\sigma) \sin \alpha}{1 + 10\varphi_2(\sigma) \sin \alpha}, \end{aligned} \tag{100}$$

where d is an arbitrary constant define parametrically three curves

$$y_i = y_i(x_i), \qquad i = 1, 2, 3,$$

which we imagine plotted on a cartesian (x, y) coordinate system. A set of values $\bar{h}$, ϵ, and σ determine three points (x_i, y_i) $(i = 1, 2, 3)$ which lie on these curves. If these points lie on a straight line, it can be shown that they satisfy (99).

On the left-hand sides of Fig. 36 we have plotted the curves given by (100) for various values of the critical angle α. The values of the parameters $\bar{h} = wh/\overline{EA}$ and ϵ, which describe the curves $y_1 = y_1(x_1)$ and $y_2 = y_2(x_2)$ respectively, are plotted on the indicated scales. Rather than indicate the values of σ along the curve $y_3 = y_3(x_3)$ we have for con-

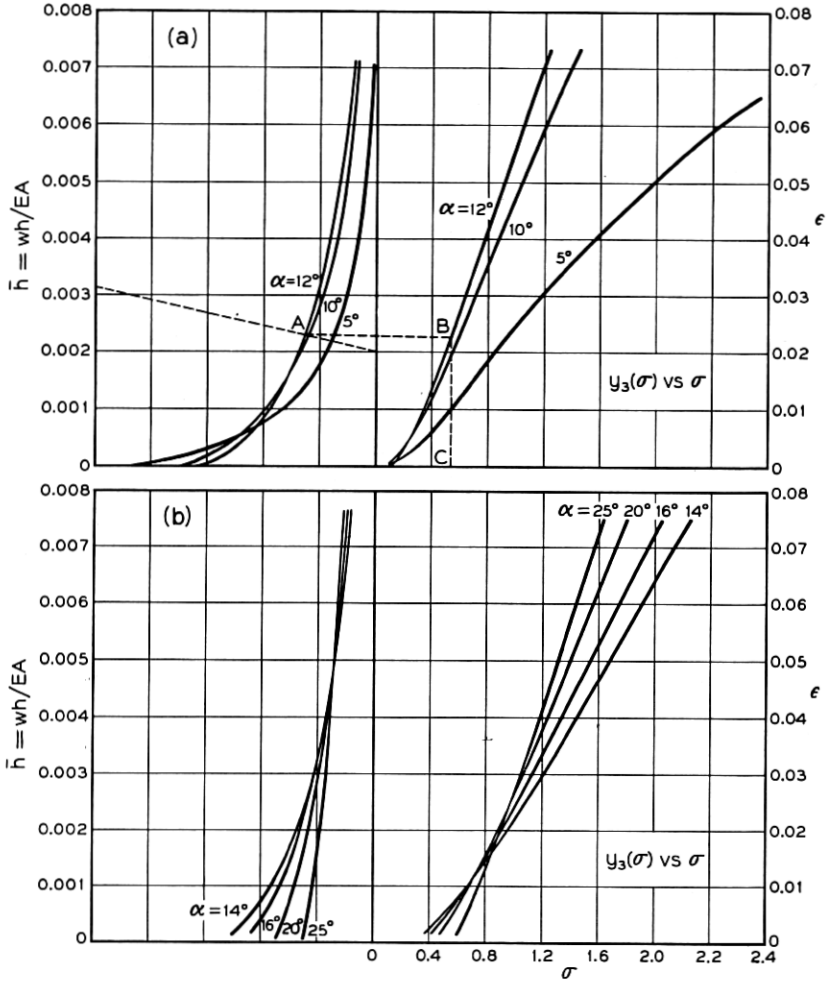

Fig. 36 — Nomograph for the solution of equation (99).

venience made an auxiliary plot on the right-hand sides of Fig. 36 of $y_3(\sigma)$ versus σ, but with numerical values of the ordinate omitted.

In addition, we have plotted in Figs. 37 and 38 the functions $1/\varphi_2$ (cosh σ) and (φ_3/φ_2) sin α for various α.

E.3 *Numerical Example*

To illustrate the method of obtaining the tension rise with time described above, we consider a numerical example for cable No. 2. The

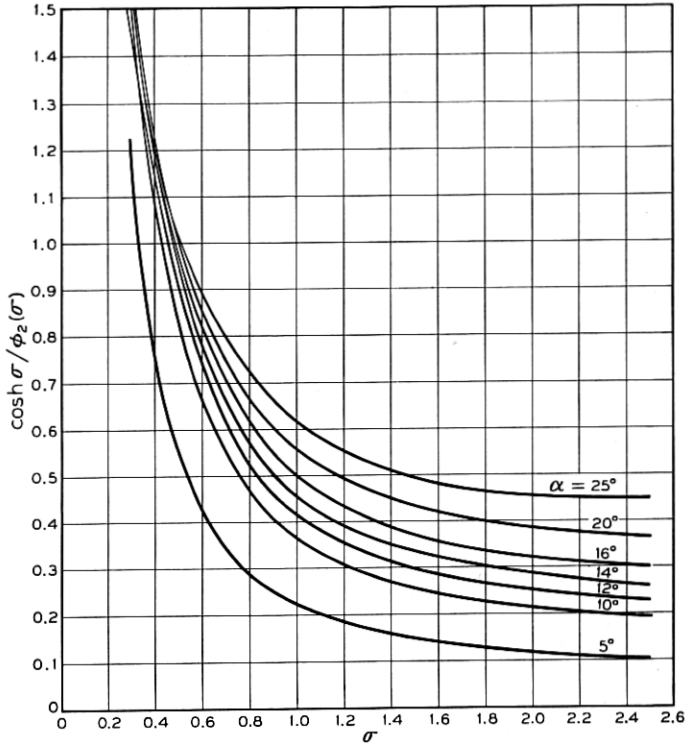

Fig. 37 — Variation of $\frac{\cosh \sigma}{\phi_2(\sigma)}$ with σ.

values we assume for the parameters which enter the calculation are the following:

$$\epsilon = 0.02,$$

$$V = 6 \text{ knots}, (\alpha \approx 12°),$$

$$h = 6{,}000 \text{ ft},$$

$$\overline{EA} = 1.2 \times 10^6 \text{ lbs},$$

$$\bar{h} = 3.1 \times 10^{-3}.$$

To solve (99), we connect on Fig. 36 the points $\epsilon = 0.02$ and $\bar{h} = wh/\overline{EA} = 0.0031$ with a straight edge and note the intersection with the intermediate $y_3 = y_3(x_3)$ curve for $\alpha = 12°$ (point A). We then locate the point on the y_3 versus σ curve having the same ordinate (point B).

Finally, we obtain the root of (99), $\sigma = 0.555$ by reading off the corresponding abscissa (point C). This value of σ now serves as the starting point in the iteration procedure by which we find the tension corresponding to a given t.

For example, for $\bar{t} = 1.0$ ($t = 600$ seconds) we have the following sequence of values

σ	$(\varphi_3 \sin \alpha)/\varphi_1$	$\bar{h}^* = \bar{h}\,[1 + (\varphi_3 \sin \alpha)\,\bar{t}/\varphi_2]$
$\sigma_0 = 0.555$	0.212	0.00379
$\sigma_1 = 0.580$	0.213	0.00380
$\sigma_2 = 0.580$		

with σ converging to the value 0.580. For $\sigma = 0.580$, Fig. 37 gives

$$\cosh \sigma/\varphi_2 = 0.800.$$

Hence, by (98b) for $\bar{t} = 1.0$

$$\bar{T}_s = 1.80,$$

and $T_s = 1.80\ wh$ or 7,600 pounds.

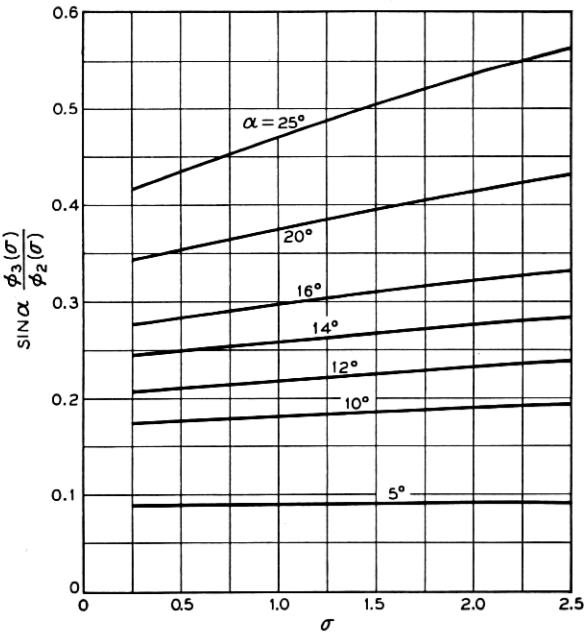

Fig. 38 — Variation of $\sin \alpha \dfrac{\phi_3(\sigma)}{\phi_2(\sigma)}$ with σ.

APPENDIX F

The Three-Dimensional Stationary Model

F.1 *Derivation of the Differential Equations*

Let $\vec{i}, \vec{j}, \vec{k}$ be unit vectors along the ξ, η, ζ axes (Fig. 26) and $\vec{t}$ a unit vector along the tangent to the cable configuration in the direction of positive s. As in the two-dimensional model, we take this to be opposite to the direction of travel of the cable elements along the configuration. With respect to the cable configuration the resultant velocity vector of the water is in the $-\vec{i}$ direction. We resolve this velocity into directions normal and tangential to the cable in the plane formed by $\vec{i}$ and $\vec{t}$. The unit vector in the normal direction we denote by $\vec{n}$, namely,

$$n = \frac{-i + (i \cdot \vec{t})\vec{t}}{|-\vec{i} + (\vec{i} \cdot \vec{t})\vec{t}|}. \tag{101}$$

In analogy to the two-dimensional model we assume the normal and tangential drag forces depend only on the corresponding water velocity components. Thus, we take

$$D_N = \frac{C_D \rho d}{2} (\vec{i} \cdot \vec{n} V)^2. \tag{102}$$

Equilibrium of the forces acting on a cable element yields the equation

$$T \frac{d\vec{t}}{ds} + \vec{t} \frac{dT}{ds} + \vec{t} D_T + \vec{n} D_N - \vec{j} w = \rho_c \vec{a}. \tag{103}$$

The vector a denotes the acceleration of an element of the cable as it moves at the constant pay-out velocity V_c along the cable configuration. It is easily shown that

$$\vec{a} = V_c^2 \frac{d\vec{t}}{ds}. \tag{104}$$

For convenience we introduce a second reference triad of orthogonal unit vectors $\vec{t}, \vec{u}$, and $\vec{v}$ as follows. The $\vec{v}$ vector is taken in the (ξ, ζ) plane normal to $\vec{t}$; the $\vec{u}$ vector is chosen equal to the vector product $\vec{v} \times \vec{t}$. The angles ψ and θ shown in Fig. 27 describe the orientation of the $(\vec{t}, \vec{u}, \vec{v})$ triad. In terms of these angles, we read from Fig. 27 the following table of direction cosines

	$\vec{i}$	$\vec{j}$	$\vec{k}$
$\vec{t}$	$\cos\theta \cos\psi$	$\sin\theta$	$-\cos\theta \sin\psi$
$\vec{u}$	$-\sin\theta \cos\psi$	$\cos\theta$	$\sin\theta \sin\psi$
$\vec{v}$	$\sin\psi$	0	$\cos\psi$

In the $(\vec{t}, u, \vec{v})$ system the vector $\vec{n}$ becomes for example

$$\vec{n} = \frac{\vec{u} \sin\theta \cos\psi - \vec{v} \sin\psi}{[\sin^2\theta \cos^2\psi + \sin^2\psi]^{\frac{1}{2}}}.$$

Imagine the origin of the $(\vec{t}, \vec{u}, \vec{v})$ triad to traverse the cable at unit velocity. The triad during this traverse rotates like a rigid body with respect to the fixed (ξ, η, ζ) frame. The rotation, which we denote by $\vec{\Omega}$, is seen from Fig. 27 to be

$$\vec{\Omega} = \vec{j}\,\dot{\psi} + \vec{v}\,\dot{\theta} = \vec{u} \cos\theta\,\dot{\psi} + \vec{v}\,\dot{\theta} + \vec{t} \sin\theta\,\dot{\psi}.$$

Here the dot denotes differentiation with respect to time, or since $ds/dt = 1$ it may be interpreted as differentiation with respect to distance along the cable. The vector $\vec{t}$ is a fixed vector of constant magnitude in the rotating $(\vec{t}, \vec{u}, \vec{v})$ triad, hence

$$\frac{d\vec{t}}{ds} = \vec{\Omega} \times \vec{t} = \vec{u}\dot{\theta} - \vec{v} \cos\theta\,\dot{\psi}. \tag{105}$$

From (101), (102), (104), and (105) we obtain for (103)

$$\begin{aligned}(T - \rho_c V_c^2)(\vec{u}\dot{\theta} - \vec{v} \cos\theta\,\dot{\psi}) + \vec{t}\left(\frac{dT}{ds} + D_T\right) \\ + \frac{C_D \rho d V^2}{2} (\sin^2\theta \cos^2\psi + \sin^2\psi)^{\frac{1}{2}}(\vec{u} \sin\theta \cos\psi - \vec{v} \sin\psi) \\ - w(\vec{u} \cos\theta + \vec{t} \sin\theta) = 0,\end{aligned} \tag{106}$$

which gives the three scalar equations, (47).

Further, let $\vec{r}(s)$ be the cable configuration, i.e.,

$$\vec{r}(s) = \vec{i}\,\xi(s) + \vec{j}\,\eta(s) + \vec{k}\,\zeta(s),$$

where $\xi(s)$, $\eta(s)$, and $\zeta(s)$ are the ξ, η, ζ coordinates of a point s of the cable. Then

$$\vec{t} = \vec{i}\,\frac{d\xi(s)}{ds} + \vec{j}\,\frac{d\eta(s)}{ds} + \vec{k}\,\frac{d\zeta(s)}{ds}.$$

Forming the scalar product of $\vec{t}$ with $\vec{i}, \vec{j}, \vec{k}$ respectively, we get (48) of Section 7.1.

In a θ, ψ, T space the solution trajectories of (47) are given by the solutions of

$$(T - \rho_c V_c^2)\frac{d\theta}{dT} = \frac{\Lambda(\cos^2\psi \sin^2\theta + \sin^2\psi)^{\frac{1}{2}} \cos\psi \sin\theta - \cos\theta}{D_T/w - \sin\theta},$$

$$(T - \rho_c V_c^2)\frac{d\psi}{dT} = \frac{\Lambda(\cos^2\psi \sin^2\theta + \sin^2\psi)^{\frac{1}{2}} \sin\psi}{\cos\theta(D_T/w - \sin\theta)}.$$

We see that the trajectories are periodic in both θ and ψ with a period of 2π, and only a single region, say

$$0 \leqq \theta \leqq 2\pi,$$

$$0 \leqq \psi \leqq 2\pi,$$

need be considered. It is apparent that the straight lines

(1) $\psi \equiv 0, \quad \theta \equiv \alpha;$ (2) $\psi \equiv 0, \quad 0 \equiv \alpha + \pi;$

(3) $\psi \equiv \pi, \quad \theta \equiv 2\pi - \alpha;$ (4) $\psi \equiv \pi, \quad \theta \equiv \pi - \alpha;$

are solution trajectories which contain all values of T. Along other solution trajectories in this region one easily verifies that

$$T = \frac{\rho_c V_c^2}{w}$$

$$\times \left(1 - \exp \int_{\theta_0}^{\theta} \frac{\left(\frac{D_T}{w} - \sin\theta\right) d\theta}{\Lambda[\cos^2\psi(\theta)\sin^2\theta + \sin^2\psi(\theta)]^{\frac{1}{2}}\cos\psi(\theta)\sin\theta - \cos\theta}\right),$$

where $\psi = \psi(\theta)$ is obtained from the solution of

$$\frac{d\psi}{d\theta} = \frac{[\cos\theta - \Lambda(\cos^2\psi\sin^2\theta + \sin^2\psi)^{\frac{1}{2}}\cos\psi\sin\theta]\cos\theta}{\Lambda(\cos^2\psi\sin^2\theta + \sin^2\psi)^{\frac{1}{2}}\sin\psi}.$$

From the definitions of ψ and θ, it follows that the lines (3) and (4) are physically identical with lines (1) and (2), and represent straight-line laying and recovery respectively. Likewise, the expression for T shows that any non-straight line trajectory with zero bottom tension is bounded by $\rho_c V_c^2/w$. Hence, as in the case of the two-dimensional model, we conclude that if the tension is somewhere greater than $\rho_c V_c^2/w$ and the bottom tension is zero, the only possible stationary configuration is the straight line lying in the plane of the resultant ship velocity and gravity vectors, and making the critical angle α with the horizontal.

F.2 *Perturbation Solution for a Uniform Cross Current*

At the outset we assume the tangential drag force to be zero. This gives by (49)

$$T = w(h + \eta), \tag{107}$$

where h is the total ocean depth. Furthermore, we take $\rho_c V_c^2$ to be zero.

If the angle φ (Fig. 26) is small compared to unity, we assume that θ and ψ will vary only slightly from the values they would have if the

upper, cross-current stratum extended all the way to the ocean bottom. That is, we take θ and ψ to be of the form

$$\begin{aligned} \theta &= \alpha' + \tilde{\theta}, \\ \psi &= \tilde{\psi}, \end{aligned} \tag{108}$$

where α' is the stationary incidence angle corresponding to the velocity V', and $\tilde{\theta}$ and $\tilde{\psi}$ are assumed small compared to unity.

Substituting (48b), (107), and (108) into (47a, b) and retaining only linear terms in θ, ψ and their derivatives, we get the linear first order equations

$$\begin{aligned} &(h + \eta)\frac{d\tilde{\theta}}{d\eta} + (2\mathrm{ctn}^2\alpha' + 1)\tilde{\theta} = 0, && \text{(a)} \\ &(h + \eta)\frac{d\tilde{\psi}}{d\eta} + \csc^2\alpha'\tilde{\psi} = 0. && \text{(b)} \end{aligned} \tag{109}$$

Because in the lower stratum the cable is a straight line parallel to the path of the ship, we have as boundary conditions:

$$\eta = -h', \begin{cases} \tilde{\theta} = \alpha - \alpha', \\ \tilde{\psi} = \varphi, \end{cases} \tag{110}$$

where h' is the depth of the upper, cross-current stratum and α is the stationary incidence angle corresponding to the velocity V.

The solution of (109) for the boundary conditions (110) is

$$\begin{aligned} \tilde{\theta} &= \left(\frac{h - h'}{h + \eta}\right)^{\mu}\Delta\alpha, \\ \tilde{\psi} &= \left(\frac{h - h'}{h + \eta}\right)^{\nu}\varphi, \end{aligned} \tag{111}$$

where

$$\begin{aligned} \mu &= (2\ \mathrm{ctn}^2\alpha' + 1), \\ \nu &= \csc^2\alpha', \\ \Delta\alpha &= \alpha - \alpha'. \end{aligned} \tag{112}$$

Equation (48) for the space-coordinates ξ, η, and ζ of the cable in turn can be written to terms of first order in the form

$$\begin{aligned} \frac{d\xi}{d\eta} &= \mathrm{ctn}\alpha' - \tilde{\theta}\csc^2\alpha', \\ \frac{d\zeta}{d\eta} &= -\tilde{\psi}\mathrm{ctn}\alpha'. \end{aligned} \tag{113}$$

Substituting (111) into (113) and integrating under the condition that at $\eta = 0, \xi = 0$ and $\zeta = 0$, we find

$$\xi = \eta \operatorname{ctn}\alpha' + \frac{(h - h')\Delta\alpha}{(\mu - 1)} \csc^2\alpha' \left[\frac{1}{(h + \eta)^{\mu-1}} - \frac{1}{h^{\mu-1}}\right],$$
$$\zeta = \operatorname{ctn}\alpha' \frac{(h - h')}{(\nu - 1)} \varphi \left[\frac{1}{(h + \eta)^{\nu-1}} - \frac{1}{h^{\nu-1}}\right]. \tag{114}$$

These equations describe the space curve formed by the cable in the cross-current stratum.

To determine the distances d and e (Fig. 32), we transform (114) for the cable configuration to coordinates ξ' and ζ' oriented along the ship's path and normal to it respectively by means of

$$\xi' = \xi \cos\varphi - \zeta \sin\varphi,$$
$$\zeta' = \xi \sin\varphi + \zeta \cos\varphi.$$

The result to terms of the first order is

$$\xi' = \eta \operatorname{ctn}\alpha' + \frac{(h - h')\Delta\alpha}{(\mu - 1)} \csc^2\alpha' \left[\frac{1}{(h + \eta)^{\mu-1}} - \frac{1}{h^{\mu-1}}\right],$$
$$\zeta' = \varphi\left(\eta \operatorname{ctn}\alpha' + \frac{\operatorname{ctn}\alpha'(h - h')}{(\nu - 1)} \left[\frac{1}{(h + \eta)^{\nu-1}} - \frac{1}{h^{\nu-1}}\right]\right).$$

Letting $\eta = -h'$ and denoting the corresponding values of ξ' and ζ' by $-d$ and $-e$ respectively, we obtain (52).

ACKNOWLEDGMENTS

Space does not allow the author to thank individually the many persons who offered comments, corrections, and information during the preparation of this paper. He is especially grateful however to C. H. Elmendorf and H. N. Upthegrove who instigated the study and provided encouragement and support during its preparation, to R. C. Prim and S. P. Morgan for critical comments on the manuscript, to B. C. Heezen for oceanographic information, to A. G. Norem, R. L. Peek, and J. F. Shea for the use of excellent unpublished earlier work on the problem, to D. Ross for assistance on cable hydrodynamics, and to N. C. Youngstrom for invaluable consultations on practical aspects of the submarine cable art and for his collaboration on the work in Appendix B.

REFERENCES

1. W. H. Thomson (Lord Kelvin), On Machinery for Laying Submarine Telegraph Cables, The Engineer, **4**, pp. 185–186, Sept. 11, 1857.

2. W. H. Thomson, Machinery for Laying Submarine Cables, The Engineer, **4,** p. 280, Oct. 16, 1857.
3. J. A. Longridge and C. E. Brooks, On Submerging Telegraph Cables, Proceedings of the Institution of Civil Engineers, pp. 269–314, Feb. 16, 1858.
4. G. B. Airy, On the Mechanical Conditions of the Deposit of a Submarine Cable, Philosophical Magazine, **16,** pp. 1–18, July, 1858.
5. W. Gravatt, On the Atlantic Cable, Philosophical Magazine, **16,** pp. 34–37, July, 1858.
6. W. S. B. Woolhouse, On the Deposit of Submarine Cables, Philosophical Magazine, **19,** pp. 345–364, May, 1860.
7. W. H. Thomson, On the Forces Concerned in the Laying and Lifting of Deep Sea Cables, *Mathematical and Physical Papers,* Vol. 2, Cambridge Univ. Press, Cambridge, 1884, pp. 153–167.
8. E. J. Routh, *Dynamics of a System of Rigid Bodies,* Vol. 2, Macmillan Co., London, 1905, pp. 401–403.
9. W. Siemens, Contributions to the Theory of Submerging and Testing Submarine Telegraphs, Journal of the Society of Telegraph Engineers, **5,** pp. 42–66, Feb. 1875. Reprinted in *Scientific and Technical Papers of Werner von Siemens,* John Murray, London, Vol. I, 1892, pp. 237–263. Also see discussions of Siemens paper in the J. of the Soc. of Telegraph Eng., **5,** by Willoughby Smith, pp. 67–76; F. C. Webb, pp. 92–97; W. Siemens, pp. 100–102; W. H. Preece, pp. 102–106; J. A. Longridge, pp. 107–112; F. C. Webb, pp. 113–115; and W. Siemens, pp. 122–126.
10. I. Brunelli, Note sur la théorie mécanique de l'immersion des câble sous-marins, Journal Télégraphique, **36,** pp. 4–6, 25–29, and 49–53, 1912.
11. L. Pode, An Experimental Investigation of the Hydrodynamic Forces on Stranded Cables, Report **713,** David W. Taylor Model Basin, Navy Department, May 1950.
12. L. Pode, Tables for Computing the Equilibrium Configuration of a Flexible Cable in a Uniform Stream, Report **687,** David W. Taylor Model Basin, Navy Department, March 1951.
13. J. W. Johnson (editor), *Proceedings of the First Conference on Ships and Waves at Hoboken, New Jersey, Oct. 1954.* Published by the Council on Wave Research and the Society of Naval Architects and Marine Engineers, 1955.
14. F. Horn, High Sea Test Trip Oscillation and Acceleration Measurements, Translation No. **26,** U. S. Experimental Model Basin, Navy Yard, Washington, D. C., March 1936.
15. F. Eisner, Das Widerstands Problem, *Third International Congress of Applied Mechanics,* Stockholm, 1930.